

## 75th Anniversary

### Historical development of the gravity method in exploration

M. N. Nabighian<sup>1</sup>, M. E. Ander<sup>2</sup>, V. J. S. Grauch<sup>3</sup>, R. O. Hansen<sup>4</sup>, T. R. LaFehr<sup>5</sup>,  
Y. Li<sup>1</sup>, W. C. Pearson<sup>6</sup>, J. W. Peirce<sup>7</sup>, J. D. Phillips<sup>3</sup>, and M. E. Ruder<sup>8</sup>



#### ABSTRACT

The gravity method was the first geophysical technique to be used in oil and gas exploration. Despite being eclipsed by seismology, it has continued to be an important and sometimes crucial constraint in a number of exploration areas. In oil exploration the gravity method is particularly applicable in salt provinces, overthrust and foothills belts, underexplored basins, and targets of interest that underlie high-velocity zones. The gravity method is used frequently in mining applications to map subsurface geology and to directly calculate ore reserves for some massive sulfide orebodies. There is also a modest increase in the use of gravity techniques in specialized investigations for shallow targets.

Gravimeters have undergone continuous improvement during the past 25 years, particularly in their ability to function in a dynamic environment. This and the advent of

global positioning systems (GPS) have led to a marked improvement in the quality of marine gravity and have transformed airborne gravity from a regional technique to a prospect-level exploration tool that is particularly applicable in remote areas or transition zones that are otherwise inaccessible. Recently, moving-platform gravity gradiometers have become available and promise to play an important role in future exploration.

Data reduction, filtering, and visualization, together with low-cost, powerful personal computers and color graphics, have transformed the interpretation of gravity data. The state of the art is illustrated with three case histories: 3D modeling of gravity data to map aquifers in the Albuquerque Basin, the use of marine gravity gradiometry combined with 3D seismic data to map salt keels in the Gulf of Mexico, and the use of airborne gravity gradiometry in exploration for kimberlites in Canada.

Manuscript received by the Editor May 9, 2005; revised manuscript received July 27, 2005; published online November 3, 2005.

<sup>1</sup>Colorado School of Mines, 1500 Illinois St., Golden, Colorado, 80401-1887. E-mail: mnabighi@mines.edu; ygli@mines.edu.

<sup>2</sup>Ander Laboratory LLC, 3604 Aspen Creek Parkway, Austin, Texas 78749. E-mail: mark@anderlab.com.

<sup>3</sup>U. S. Geological Survey, Box 25046, Federal Center MS 964, Denver, Colorado 80225. E-mail: tien@usgs.gov; jeff@usgs.gov.

<sup>4</sup>PRJ Inc., 12640 W. Cedar Dr., Suite 100, Lakewood, Colorado 80228. E-mail: rohansen@prj.com.

<sup>5</sup>Colorado School of Mines (retired), 1500 Illinois Street, Golden, Colorado 80401-1887. E-mail: lafehr@bresnan.net.

<sup>6</sup>Pearson Technologies Inc., 1801 Broadway, Suite 600, Denver, Colorado 80202. E-mail: bpearson@pearsontechnologies.com.

<sup>7</sup>GEDCO, 815 Eighth Ave. S.W., Calgary, Alberta T2P 3E2, Canada. E-mail: jwpeirce@gedco.com.

<sup>8</sup>Wintermoon Geotechnologies, Inc., 280 Columbine, Suite 301, Denver, Colorado 80206. E-mail: meruder@wintermoon.com.

© 2005 Society of Exploration Geophysicists. All rights reserved.

## HISTORICAL OVERVIEW

Modern gravity exploration began during the first third of the twentieth century and continues to this day as a small but important element in current exploration programs (Appendix A). The first geophysical oil and gas discovery, the Nash dome in coastal Texas, was the result of a torsion-balance survey (LaFehr, 1980). A historical outline of the early development of the gravity method of exploration, from pendulums to torsion balances to gravimeters, is given by Eckhardt (1940).

Recent reviews (LaFehr, 1980; Paterson and Reeves, 1985; Hansen, 2001) document the continuous evolution of instruments, field operations, data-processing techniques, and methods of interpretation and refer to unpublished works to help provide an accurate understanding of the usefulness of gravity and magnetic methods. They also comment on the state of the geophysical literature, which allows mathematical sophistication to overshadow geologic utility (LaFehr, 1980; Paterson and Reeves, 1985). A steady progression in instrumentation (torsion balance, a very large number of land gravimeters, underwater gravimeters, shipborne and airborne gravimeters, borehole gravimeters, modern versions of absolute gravimeters, and gravity gradiometers) has enabled the acquisition of gravity data in nearly all environments, from inside boreholes and mine shafts in the earth's shallow crust to the undulating land surface, the sea bottom and surface, in the air, and even on the moon. This has required a similar progression in improved methods for correcting for unwanted effects (terrain, tidal, drift, elevation, and motion-induced) and the parallel increase in precision of positioning data.

One of the pleasant surprises in recent exploration history has been the marked improvement in gravity data acquired aboard 3D seismic vessels. In combination with better control systems, closely spaced seismic traverses, and larger, more stable ships, the quality of marine gravity data acquired at the sea surface now surpasses underwater gravity accuracy, a claim that could not have been made in 1980. And of course, modern global positioning system (GPS) instrumentation and data processing have significantly increased accuracies.

Gravity interpreters have been able to take advantage of these improvements in data acquisition and processing because of the wide availability of inexpensive workstations and personal computers. Significant early contributions (e.g., Skeels, 1947; Henderson and Zietz, 1949; Bhattacharyya, 1967; Fuller, 1967; Bhattacharyya and Chan, 1977) are still relevant today. The fundamentals of interpretation are the same today as they were 25 years ago, but GPS and small, powerful computers have revolutionized the speed and utility of the gravity method. With the availability of software running on laptop computers rather than mainframes or UNIX-based workstations, data are acquired automatically and even processed and interpreted routinely in the field during data acquisition. Information can now be transmitted from the field via satellite link, stored on centralized data servers, and retrieved on the Web. In hydrocarbon exploration, seismic models derived from prestack depth migration are routinely used as input to gravity modeling, and the latter is being used to further refine seismic depth and velocity models.

## APPLICATIONS OF GRAVITY MEASUREMENTS

Gravity measurements are used at a wide range of scales and purposes. On an interstellar scale, understanding the shape of the gravity field is critical to understanding the nature of the space-time fabric of the universe. On a global scale, understanding the details of the gravity field is critical in military applications which, since World War II, have stimulated much of the research and development in the areas of gravity instrumentation and building global databases. On an exploration scale, the gravity method has been used widely for both mining and oil exploration, and at the reservoir scale it is used for hydrocarbon development.

The use of gravity for exploration has included all manner of targets, beginning with the use of the torsion balance in exploring for salt domes, particularly on the U. S. Gulf Coast. The methodology was so integral to oil exploration that from 1930 to 1935, the total number of gravity crews exceeded the total number of seismic crews (Ransone and Rosaire, 1936). With the advent of more practical field instruments (see section titled History of Gravity Instrumentation), the use of gravity techniques rapidly expanded in both mining and hydrocarbon exploration for any targets for which there was a density contrast at depth, such as salt domes, orebodies, structures, and regional geology.

Gravity measurements for exploration were often made on a relative basis, where an arbitrary datum for a particular survey was established and all values were mapped relative to it. In 1939, George P. Woollard (1943) undertook a series of gravity and magnetic traverses across the United States with observations at 10-mile intervals to determine the degree to which regional geologic features were reflected in the data (Woollard and Rose, 1963). As coverage expanded in the 1940s, the need became apparent to establish a regional set of datum references, all tied back to the reference measurement of the absolute gravity field of the earth in Potsdam, Germany. This led to a program started in 1948 by the U. S. military to test the reliability of the world network of first-order international gravity bases and to simultaneously build up a secondary network of gravity control bases at airports throughout the world (Woollard and Rose, 1963). The final result was the establishment of the International Gravity Standardized Network (IGSN) (Morelli, 1974; Woollard, 1979), to which almost all modern gravity measurements are now tied.

Unlike seismic data, land and underwater gravity data seldom are outdated because the basic corrections have not changed significantly over the years. In older foothills data, the terrain corrections can be updated with modern digital elevation models, but the basic data are still valuable if the original position quality was good and the original observed gravity values are still available. However, modern airborne gravity surveys do offer the possibility of collecting much more evenly spaced data that can alleviate serious problems with spatial aliasing associated with irregularly spaced ground stations (Peirce et al., 2002).

With the advent of gravity measurements derived from satellite altimetry (see Satellite-derived Gravity), the density of gravity measurements in the oceans took a quantum leap forward. Many details of the geometry of tectonic plates, particularly in the southern hemisphere, became clear for the first time. In the 1980s, large national gravity databases

became available for many continents, leading to many studies of continental tectonics (e.g., Hinze, 1985; Sharpton et al., 1987; Chapin, 1998a; Gibson, 1998). Studies of flexure and subsidence on continental margins (e.g., Watts and Fairhead, 1999) incorporated gravity data as a major constraint.

Historically, gravity has been used in oil exploration in any plays involving salt because of the large density contrast of salt, at almost all depths, with surrounding sediments (positive when shallow, negative when deep; e.g., Greene and Bresnahan, 1998). A very large effort has been made in the U. S. Gulf of Mexico to use gravity modeling as a constraint for seismic imaging of the bottom of allochthonous salt bodies. The gravity data are used in conjunction with prestack depth migration of the seismic data in an iterative way to build a better velocity cube, thereby leading to clearer images of the base of the salt (Huston et al., 2004; see Case History). For interpretations of this type, gravity gradiometry data are preferred because of their higher resolution in the upper sedimentary section. Interpreting such data requires a modeling package that can handle multicomponent gravity tensors (Pratson et al., 1998; O'Brien et al., 2005).

Gravity techniques have been used for many years to map the geometry and features of remote basins (e.g., Paterson and Reeves, 1985; Peirce and Lipkov, 1988; Pratsch, 1998; Jacques et al., 2003). Much of the recent work has been done using airborne gravity (e.g., Ceron et al., 1997), but most of that remains unpublished. With the dramatic improvements of the resolution of airborne gravity and gradiometry with GPS navigation, airborne gravity is now used much more widely in mining (Liu et al., 2001; Elieff, 2003; Elieff and Sander, 2004) as well as in hydrocarbon exploration on a more target-specific basis, e.g., surveys in offshore Mexico and in the foothills environment (Peirce et al., 2002).

On a reservoir scale, borehole gravimeters (BHGM) have been used extensively to detect porosity behind pipes or to more accurately measure bulk density for petrophysical uses (see "Borehole Gravity Instruments") as well as for sulfur exploration (Alexander and Heintz, 1998). Today, absolute gravity measurements are an additional constraint in monitoring water injection during secondary recovery on the North Slope of Alaska (Brown et al., 2002). Gravity measurements have also received limited use as an alternative means of estimating static corrections for seismic data (Opfer and Dark, 1989).

In the mining industry, gravity techniques are still widely used as an exploration tool both to map subsurface geology and to help estimate ore reserves for some massive sulfide orebodies. In addition, the gravity method is sometimes applied to specialized shallow applications, including archaeology (Lakshmanan and Montlucon, 1987; Deletie et al., 1988; Brissaud et al., 1989), weapons inspection (Won et al., 2004), detecting shallow mine adits in advance of housing developments (Ebner, personal communication, 1996), and detecting faults and paleochannels in hydrologic investigations (Hinze, 1991; Grauch et al., 2002; see also Case History).

## HISTORY OF GRAVITY INSTRUMENTATION

Gravity sensors fall into one of two categories: absolute or relative. An absolute gravity instrument measures the local value of gravity each time it makes a measurement.

A relative gravity instrument measures the difference in gravity between measurements. A relative instrument is all that is usually required for most exploration purposes. In general, absolute gravity instruments typically are far more expensive, are much bigger, take much longer to make a high-precision measurement, and require more knowledge and skill to use than do relative gravity instruments.

The historical advancement of gravity instrumentation has been driven by a combination of increased precision, reduced time for each measurement, increased portability, and a desire for automation and ease of use. Hundreds of different designs of gravity sensors and gravity gradiometers have been proposed or built since the first gravity measurements were made. Given the relative size and importance of gravity exploration compared to seismic exploration, it is impressive to realize that about 40 different commercial gravity sensors and gravity gradiometers are available (Chapin, 1998b) and about 30 different gravity sensor and gravity gradiometers designs have either been proposed or are under development. Even so, only six general types of gravity and gravity gradiometry sensors have been widely used for geophysical exploration at different times: the pendulum, the free-fall gravimeter, the torsion-balance gravity gradiometer, the spring gravimeter, the vibrating-string gravimeter, and the rotating-disk gravity gradiometer. These instruments have been adapted at various times for land, borehole, marine, submarine, ocean-bottom, airborne, space, and lunar surveying.

## Pendulums

For more than two millennia, the widely accepted theory of gravity, as described by Aristotle (384–322 BC), was that the velocity of a freely falling body is proportional to its weight. Then in 1604 Galileo Galilei, using inclined planes and pendulums, discovered that free fall is a constant acceleration independent of mass. In 1656, Christian Huygens developed the first pendulum clock and showed that a simple pendulum can be used to measure absolute gravity,  $g$ . To make an absolute measurement of  $g$  to a specified precision, the moment of inertia  $I$ , the mass, the length  $h$ , and the period of the pendulum must be known to the same degree of precision. A desirable precision would be better than 1 ppm of the earth's gravity field. Until the beginning of the 20th century, it was virtually impossible to measure  $h$  or  $I$  with any great precision. Consequently, before the 20th century, using a pendulum to make an absolute measurement resulted in precisions of about 1 Gal ( $10^{-2}$  m/s<sup>2</sup>). However, it is easier to use a pendulum as a much higher precision-relative instrument by measuring, with the same pendulum, the difference in gravity between two locations. Pendulums were used as relative instruments throughout the 18th and 19th centuries as scientists began mapping the position dependency of gravity around the earth.

In 1817, Henry Kater invented the reversible pendulum by showing that if the period of swing was the same about each of the points of support for a pendulum that could be hung from either of two points, then the distance separating these points of suspension was equal to the length of a simple pendulum having the same period (Kater, 1818). Thus, the problem reduced to measuring the common period and the distance separating the two supports. Reversible pendulums were a substantial improvement in absolute gravity measurement, with

an initial precision of about 10 mGal ( $10^{-4}$  m/s<sup>2</sup>). Over the next 100 years, several incremental improvements to the reversible pendulum culminated with Helmert's substantial revision of the theory of reversible pendulums (Helmert, 1884, 1890), which brought its absolute gravity measurement precision to about 1 mGal ( $10^{-5}$  m/s<sup>2</sup>). Between 1898 and 1904, Kühnen and Furtwängler performed absolute gravity measurements to this precision in Potsdam, which became the base for the Potsdam Gravity System, introduced in 1908 and later extended worldwide by converting previous gravity measurements to this datum (Torge, 1989).

In the first half of the 1900s, several different pendulums were in use, including Sterneck's pendulum developed in 1887 (Swick, 1931), the Mendenhall pendulum developed in 1890 (Swick, 1931), the first pendulum developed for use in a submarine by Vening Meinesz (Meinesz, 1929), the Gulf pendulum developed in 1932 (Gay, 1940; Wyckoff, 1941), and the Holweck-Lejay pendulum (Dobrin, 1960). Sterneck's pendulum was used primarily as a relative instrument. With the exception of the Gulf pendulum, these pendulums were used almost exclusively for geodetic purposes. The Gulf pendulum, developed by Gulf Research and Development Company, was used extensively for oil exploration for about 10 years with data collected from more than 8500 stations along the U. S. Gulf Coast (Gay, 1940). [For further discussions of pendulum instruments, see Heiskanen and Meinesz (1958) and Torge (1989).]

### Free-fall gravimeter

Free-fall gravimeters have advanced rapidly since they were first developed in 1952. The method involves measuring the time of flight of a falling body over a measured distance, where the measurements of time and distance are tied directly to internationally accepted standards. The method requires a very precise measurement of a short time period, which only became possible with the introduction of the quartz clock in the 1950s. The first free-fall instruments used a white-light Michelson interferometer, a photographic recording system, a quartz clock, and a falling body, typically a 1-m-long rod made of quartz, steel, or invar. The final value of gravity was obtained by averaging 10 to 100 drops of several meters. These first instruments had a crude resolution of greater than 1 mGal.

By 1963, the use of a corner-cube mirror for the falling body, a laser interferometer, and an atomic clock substantially improved the sensitivity of free-fall instruments. A second corner cube was fixed and used as a reference. A corner-cube mirror always reflects a laser beam back in the direction from which it came, regardless of the orientation of the corner cube. A beam splitter divides the laser beam into a reference beam and a measurement beam, each beam forming an arm of the Michelson interferometer. Each beam is reflected directly back from its respective corner cube and again passes through the beam splitter, where it is superimposed to produce interference fringes at a photo detector; the fringe frequency is proportional to the velocity of the falling body.

By the early 1970s, the best measurements were in the range of 0.01 to 0.05 mGal, and by about 1980, free-fall gravimeters had replaced pendulums for absolute gravity measurements. Over time, the falling distances became shorter and the number of drops increased, making the instruments more

portable. The only commercially available free-fall gravimeters are manufactured by Micro-g Solutions, Inc., and are capable of a resolution of about 1  $\mu$ Gal, which rivals the sensitivity of the best relative spring gravimeters. Their disadvantages are that they are still larger, slower, and much more expensive than relative gravimeters. Micro-g Solutions has built about 40 absolute free-fall gravimeters. [For reviews of free-fall gravimeters, see Torge (1989), Brown et al. (1999), and Faller (2002).]

### Torsion-balance gravity gradiometer

Starting in 1918 and continuing to about 1940, the torsion-balance gravity gradiometer, developed by Baron Roland von Eötvös in 1896, saw extensive use in oil exploration. It was first used for oil prospecting by Schweydar (1918) over a salt dome in northern Germany and then in 1922 over the Spindletop salt dome in East Texas. The sensitivity, accuracy, and relative portability of the torsion balance made it the most useful gravity exploration technology of its era. By 1930, about 125 of these instruments were being used in oil exploration worldwide. Several different torsion-balance designs were developed by various manufacturers, including Askania in Berlin and Suess in Budapest.

The Eötvös torsion balance consists of a vertically suspended torsion fiber, usually made of platinum-iridium or tungsten, with a horizontal aluminum bar suspended from its lower end. One end of the bar carries a proof mass, usually made of platinum or gold, and the other end carries an identical proof mass suspended by another fiber several centimeters below the horizontal plane of the bar. The balance bar rotates when a differential horizontal force acts on the two masses, which happens when the earth's gravitational field in the neighborhood of the balance is distorted by mass differences at depth, such that the horizontal component of gravity at one proof mass is different from that at the other proof mass. The horizontal movement of the bar twists the torsion fiber until the resistance to torsion becomes equivalent to the torque of rotation and the bar comes to rest. The magnitude of the torque can be determined by measuring the angle through which the balance has been rotated by the torque. The angular displacement is measured optically by a mirror mounted in the vertical axis of rotation of the balance bar and reflects an image of a fixed scale to a fixed telescope or reflects a fixed beam of light to a fixed photographic plate. Because the proof masses are suspended from the torsion fiber at unequal heights, one can measure two components of the gravity gradient: the horizontal gradient perpendicular to the horizontal component of the field (the torsion), which is what can be obtained with masses at equal heights (effectively a Cavendish balance), and the difference between the two inline horizontal gradients, a quantity known as the curvature because it is the difference between the two sectional curvatures of the potential in the horizontal plane. [Detailed discussions can be found in Rybar (1923) and Barton (1928).]

With careful measurement procedures, accuracies of a few Eötvös units ( $IE = 10^{-9} \text{ S}^{-2} \text{ mGal/km}$ ) could be obtained; but in field operations a torsion balance typically took about three to six hours to obtain a gravity station, including setup and teardown, so four to eight stations per day could be surveyed. The instrument was placed inside a tent during measurements

to protect it from the perturbing influences of wind and solar radiation.

In general, gravity gradiometers, including the torsion balance, are more sensitive to near-sensor mass changes than are gravity sensors. As a consequence, gravity gradiometers have a significant advantage over gravimeters in sensing topographic effects in land and airborne environments or bathymetric effects in marine environments. But if mass changes exist close to a gradiometer, this sensitivity can mask gravity gradient signals from deeper structures. In the 1920s and 1930s, terrain mapping was not as sophisticated as it is today; as a consequence, the torsion balance could only be used in relatively flat areas, e.g., less than 3 m of elevation change within 100 m of the station. Although the instrument had a precision of approximately 1–3 EU, uncertainties in terrain plus influences of the mass of the observer limited the practical field resolution to about  $\pm 10$  EU. Today, modern gravity gradiometers are coupled with high-resolution terrain or bathymetric mapping to take advantage of the tool's sensitivity to nearby masses.

The torsion balance became obsolete with the development of spring gravimeters, although the Geophysical Institute in Budapest continued to develop the torsion balance into the 1950s (J. Rybar, 1957). The compact spring gravimeter proved to be a portable, rugged, and robust instrument, capable of taking dozens of measurements daily.

### Spring gravimeters

Spring gravimeters measure the change in the equilibrium position of a proof mass that results from the change in the gravity field between different gravity stations. This measurement can be accomplished in one of three ways:

- 1) measuring the deflection of the equilibrium position (typically done mechanically by measuring the deflection of a light beam reflected off a mirror mounted on or connected to the proof mass);
- 2) measuring the magnitude of a restoring force (typically using a capacitive feedback system but a magnetic system also works) used to return the equilibrium position to its original state;
- 3) measuring the change in a force (typically capacitive feedback) required to keep the equilibrium position at some predefined null point.

Historically, spring gravimeters have been classed as stable or unstable. For stable gravimeters, the displacement of the proof mass is proportional or approximately proportional to the change in gravity. An example of a stable gravimeter is a straight-line gravimeter. For unstable gravimeters, the displacement of the proof mass introduces other forces that magnify the displacement caused by gravity and hence increase system sensitivity. Examples of unstable instruments are those with inclined zero-length springs, such as the LaCoste & Romberg (L&R) G-meters, the Worden meter, and the Scintrex meter.

Most spring gravimeters use an elastic spring for the restoring force, but a torsion wire may also be used. The theory and practical understanding of such instruments has been known

since Robert Hooke formulated the law of elasticity in 1678, and various spring balance instruments have been in practical use since the start of the 18th century. John Hershel first proposed using a spring balance to measure gravity in 1833. But it was not until the 1930s that demands of oil exploration, which required that large areas be surveyed quickly, and advances in material science led to the development of a practical spring gravimeter.

The simplest design is the straight-line gravimeter, which consists of a proof mass hung on the end of a vertical spring. Straight-line gravimeters are used primarily as marine meters. The first successful straight-line marine gravimeter was developed by A. Graf in 1938 (Graf, 1958) and was manufactured by Askania. L&R also manufactured a few straight-line marine gravimeters.

To obtain the higher resolution required for land gravimetry, a more sophisticated spring balance system was developed, involving a mass on the end of a lever arm with an inclined spring. The added mechanical advantage of the lever arm increased sensitivity by a factor of up to 2000. The first such system, developed by O. H. Truman in 1930, was manufactured by Humble Oil Company and had a sensitivity of about 0.5 mGal.

Between 1930 and 1950 more than 30 types of spring gravimeter designs were introduced, but by far the most successful was developed in 1939 by Lucien LaCoste and was manufactured by L&R. Since then, L&R has built more than 1200 G and 232 two-screw D-meters for use on land, 142 air/sea meters for use on ships and airplanes, about 20 ocean-bottom meters, 16 borehole gravity meters, and 2 moon meters, one of which was deployed during the Apollo 17 mission (the moon meter did not work).

The key to the L&R sensor was the zero-length spring invented by LaCoste (LaCoste, 1934). The zero-length spring made relative gravimeters much easier to make, calibrate, and use (LaCoste, 1988). The L&R gravity sensor makes routine relative gravity measurements to an accuracy of about 20  $\mu$ Gal without corrections for instrument errors (Valliant, 1991) and, with great care taken in correcting for both instrumental and external errors, down to 1–5  $\mu$ Gal in the field and 0.2  $\mu$ Gal in a laboratory (Ander et al., 1999). To obtain a high precision, range changing must not be performed and system corrections must be adjusted for temperature and pressure changes, sensor drift (primarily spring hysteresis and creep), and vibration. LaCoste's creative genius dominated the field of gravity instrumentation for more than half a century (Clark, 1984; Harrison, 1995).

In 1948, Sam Worden of Worden Gravity Meter Company introduced an inclined zero-length spring gravimeter that uses a spring made of fused quartz. The Worden system configuration is similar to the L&R meter except that it uses a lighter proof mass (5 mg) than the L&R instrument (15 grams). Worden enclosed his sensor in a vacuum flask, which greatly reduces the instrument's temperature and pressure sensitivity. As a result, the Worden meter is smaller, lighter, and faster and uses less power than the L&R meter. The practical sensitivity of the Worden meter is about 0.01 mGal. There are several advantages and disadvantages to using a quartz spring rather than a metal spring. Quartz springs are easier and faster to manufacture than metal springs; metal springs fatigue, and quartz springs do not. However, quartz springs are much more

fragile than metal springs, and over time, quartz can crystallize and hydrolyze.

The Worden meter is still in production, with more than 1000 meters built. Two other gravimeter companies, Soden Ltd. and Scintrex Ltd., have also built quartz zero-length spring gravimeters. In 1989, Andrew Hugill at Scintrex Ltd. developed a gravity sensor made of fused quartz with capacitive displacement sensing and automatic electrostatic feedback. The CG-3 and later the CG-5 gravimeters were the first self-leveling instruments; as a result, over the next ten years Scintrex gravimeters became a major competitor of L&R meters.

In 1999, Mark Ander led a team that developed the automated L&R Graviton EG<sup>TM</sup> meter using an onboard microprocessor combined with a capacitive force feedback system that eliminated the need for a zero-length spring. The capacitive force feedback system forces the sensor to remain at a horizontal reference position; gravity is determined by the amount of capacitive force required to keep the proof mass at the reference position. In the Graviton EG meter, the mechanism is in place to make it an unstable gravimeter, but because the proof mass does not move away from the null point, it is neither a stable nor an unstable gravimeter. L&R discontinued their D-meter in 1999 and their G-meter in 2004.

Most commercially available relative gravimeters made today use a zero-length spring made either of metal (L&R and Zero Length Spring Inc.) or quartz (Scintrex Ltd., Worden Gravity Meter Company, and Soden Ltd.). [For a review of various designs of spring sensors see Torge (1989).]

### Gravimeter gradiometry

As targets became smaller and were characterized by more subtle gravity signatures, new interest arose in mapping gravity gradients directly in the field. The benefit of this approach was improved spatial resolution and sensitivity of the gradient signal compared to the vertical component of the gravity field. Starting in the 1950s, spring gravimeters were used to determine small gravity differences to approximate the horizontal and vertical gravity gradients. To measure the vertical gradient, a specially designed tripod can be used to make gravity-difference measurements with separations of up to 3 m. A precision of 10 to 30 EU can be achieved using this method (Götze et al., 1976). Vertical gravity differences have also been measured in buildings and tall towers with varying degrees of success. Horizontal gravity gradients can be approximated using gravity data taken along a horizontal profile with a station spacing of 10 to 50 m and correcting for any height adjustments (Wolf, 1972). Although these methods were never extensively practiced, they are still in use today.

### Vibrating-string gravimeter

The first vibrating-string gravimeters were developed by Gilbert (1949) for use on submarines and were later adapted for use in marine, land, and borehole applications. These gravimeters have the advantage of generally being physically smaller than spring gravimeters but with a larger dynamic range. String gravimeters use the transverse oscillation of a vertically suspended elastic string with a mass on the end. The string is made of an electrically conducting material that oscil-

lates at its resonant frequency in a magnetic field. This configuration generates an oscillating voltage of the same frequency that is amplified and used in a feedback system to further excite the string.

Vibrating-string gravimeters can be designed with several different string and mass configurations. The simplest is a vertically suspended string with a freely suspended mass on the end, where the frequency of vibration is directly proportional to the square root of the gravity field. The second is a vertically suspended string-mass system that is constrained at both ends. Such a system was used in the Tokyo surface-ship gravity meter developed in the early 1960s and used extensively for marine gravity acquisition (Tomoda et al., 1972). The third and most complicated is a vertically suspended double string and double mass system, where the second string and mass are mounted below the first string and mass using a weak spring, and the entire system is constrained at both ends. In this system, a change in gravity causes a change in the tension of the two strings, resulting in a difference between the natural frequencies of the two strings that is proportional to the change in gravity. Cross-coupling effects typically associated with gravity measurements on moving platforms can be largely eliminated by the use of cross-support ligaments. This particular configuration was first developed in the Massachusetts Institute of Technology (MIT) vibrating-string accelerometer (Wing, 1969).

Since 1967, this system has been used for marine gravity surveys by the Woods Hole Oceanographic Institution and by the University of Wisconsin (Bowin et al., 1972). Vibrating-string instruments had also been developed in the former Soviet Union for land and marine exploration and are still in use in Russia and China (Lozhinskaya, 1959; Breiner et al., 1981). In 1973, a double-string and double-mass vibrating-string sensor developed by Bosh-Arma was used to successfully obtain gravity measurements on the moon during the Apollo 17 mission (Chapin, 2000; Talwani, 2003). This is the only time that successful gravity measurements have been made by man on a celestial body other than earth.

### Borehole gravity instruments

Borehole gravity meters (BHGMs) were first developed in the late 1950s in response to the petroleum industry's need for accurate downhole gravity data to obtain formation bulk density as a function of depth.

The first instrument to measure gravity in a borehole was developed by Esso for oil exploration (Howell et al., 1966). It used a vibrating-filament sensor, where the frequency of vibration was related to the tension on the filament, and the frequency changed as gravity varied. This instrument had a resolution of about 0.01 mGal with a reading time of about 20 min. It was thermostatically controlled to operate up to 125°C, but it could only operate at less than 4° from vertical. A short time later, L&R miniaturized and adopted its land G-meter into a logging sonde to produce its BHGM. The L&R BHGM can make routine borehole gravity measurements with a resolution of 5 to 20  $\mu$ Gal and, with care, to 1  $\mu$ Gal. Therefore, the L&R BHGM can detect many important fluid contacts behind pipe because most gas-water and gas-oil contacts are resolvable between 2 and 5  $\mu$ Gal, and most oil-water contacts are resolvable between 0.7 and 3  $\mu$ Gal.

The L&R BHGM is thermostatically controlled to operate at temperatures up to 125°C. It can only access well casings with at least a 5 1/2-in diameter, and it can only make gravity measurements up to 14° from vertical, which severely limits access to petroleum wells and gives almost no access to mining boreholes. Despite its severe limitations, the L&R BHGM has proven to be a valuable tool in a variety of applications. L&R manufactured 16 BHGMs, of which 13 still exist today.

### Underwater gravity instruments

In the 1940s, extensive seafloor gravity measurements were made for oil exploration in the Gulf of Mexico using specially designed diving bells developed by Robert H. Ray Company (Frowe, 1947). Diving operations were hazardous; therefore, remote-control underwater gravimeters were created. The underwater gravimeters consist of a gravity sensor, a pressure housing, a remote control and display unit on the vessel, an electronic cable connection, and a winch with a rope or cable to lower and raise the system. In addition, the system remotely levels, clamps/unclamps, reranges, and reads the sensor. The sensor must be strongly damped to operate on the ocean bottom.

One of the first ocean-bottom systems was the Gulf underwater gravimeter (Pepper, 1941). Ocean-bottom gravimeters have also been built by Western and by L&R. The L&R U-meter is the most popular underwater gravimeter today and has a maximum depth of about 60 m. Underwater gravity measurements have accuracies on the order of 0.01 to 0.3 mGal, depending on sea state, seafloor conditions, and drift rate control, with survey rates on the order of 10 to 20 stations per day, depending on the depth of the measurement and the distribution of stations.

An adaptation of the underwater meter was the long-line system developed by Airborne Gravity Ltd. It was designed to operate remotely on a cable suspended from a helicopter. This allowed surveying in rough or forested terrain without having to land the helicopter. Scintrex developed a similar system for their meters.

### Moving-platform gravity instruments

Large areas can be covered quickly using gravity sensors attached to moving platforms such as trucks, trains, airplanes, helicopters, marine vessels, or submarines. In such systems, large, disturbing accelerations result from vehicle motion and shock and are a function of (1) external conditions such as wind, sea state, and turbulence; (2) the platform type and model; (3) the navigational system; and (4) the type and setup of the gravimeter.

The primary factor limiting moving-platform gravity measurement resolution is how well the external accelerations are known, particularly vertical acceleration, because the vertical component of acceleration adds directly to the gravity measurement. The other components of acceleration couple differently to the gravity sensor. The horizontal components of acceleration, depending on their orientation to the gravity sensor and the orientation of the gravity sensor to vertical, will have a more indirect and damped effect on gravity measurements and may exhibit cross-coupling effects. In cross-coupling, which depends on instrument design, components of horizontal acceleration couple through the instrument to

produce an effect similar to vertical acceleration. In addition, corrections must also be made for Coriolis acceleration, resulting from the direction of the moving platform relative to the rotation of the earth. Finally, all platforms are subject to high-frequency vibrations.

Gravity measurements on moving platforms are made primarily with spring gravimeters; vibrating-string and force-balanced accelerometers are used much less, particularly in airborne systems. The gravity sensor and the setup must be heavily damped against vibrations. Setup includes platform stabilization such as a gyrostabilizer or gimballed suspension. Low-pass filtering is typically applied to minimize the effect of high-frequency accelerations of the platform. On marine vessels, vertical accelerations can have effects as large as 105 mGal, with frequencies from 0.05–1 Hz. On an aircraft, the effects are on the order of 20 000 mGal but have a broader frequency range of 0.002–1 Hz. In addition, airborne gravimeters require short averaging times because of their high relative velocities.

The first shipborne gravity instruments were gas-pressured gravimeters, developed in 1903 and used until about 1940. They used atmospheric pressure as the counterforce to gravity acting on the mass of a mercury column (Hecker, 1903; Haalck, 1939). Extensive gravity measurements began in submarines starting in 1929 when Vening Meinesz modified a pendulum to operate on a submarine (Meinesz, 1929). This instrument was used in submarines until about 1960 and had a precision of about 2 mGal. The first marine spring gravimeter was the straight-line marine gravimeter developed by A. Graf in 1938 (Graf, 1958) and manufactured by Askania as the Seagravimeters Gss2 and Gss3. This instrument was used from 1939 to the 1980s and had a precision of about 1 mGal (Worzel, 1965). The L&R spring gravimeters were first modified for use on a submarine in 1954 (Spiess and Brown, 1958) and then on a ship in 1958 (Harrison, 1959; LaCoste, 1959). In 1959, an L&R gravimeter was used to make the first airborne gravity measurement tests (Nettleton et al., 1960; Thompson and LaCoste, 1960). In 1965, L&R developed its S-meter, a stabilized-platform gravimeter for use on ships and in airplanes (LaCoste, 1967; LaCoste et al., 1967). The first helicopter gravity surveys using the S-meter were made in 1979 and were accurate to about 2 mGal. Then in the mid-1980s, the S-meter was adapted for use in deep-sea submersibles (Luyendyk, 1984; Zumberge et al., 1991). Today, the L&R air-sea gravimeter, which uses a gyroscopically stabilized platform, is the most widely used moving-platform gravimeter, with 142 systems built since 1967. Another important system is the Bodenseewerk improved version of the Askania Gss2, the KSS30.

Carson Services, Inc., has offered airborne gravity surveys using L&R meters in helicopters and Twin Otters since 1978. The advent of GPS dramatically improved accuracy, and several companies offered airborne gravity services in fixed-wing aircraft. A series of unfortunate plane crashes caused a major reevaluation of safety procedures, resulting in the creation of the International Airborne Geophysics Safety Association (IAGSA) in 1995 and a realignment of the airborne gravity business. In 1997, Sander Geophysics developed its AirGrav airborne inertially referenced gravimeter system based on a three-axis accelerometer with a wide dynamic range. The system has extremely low cross-coupling. Sander Geophysics has

built four AirGrav systems so far. A Russian system that uses accelerometers has been introduced recently by Canadian MicroGravity, and two of these systems are being operated by Fugro Airborne Surveys. Today, airborne gravity surveying is offered by several companies, including Carson, Fugro, and Sander Geophysics.

Currently, the best commercial marine gravity measurements have a resolution of about 0.1 mGal over not less than 500-m half-wavelength. The best commercial airborne gravity measurements have a resolution of better than 1 mGal over not less than 2-km half-wavelength from an airplane and better than 0.5 mGal over less than 1-km half-wavelength from a helicopter. These performance figures are hotly debated, and it is often difficult to find comparable data from different companies because there are many ways to present resolution performance. [A thorough discussion of gravimetry applied to moving platforms can be found in Torge (1989).]

### Rotating-disk gravity gradiometers

Since World War II, gravity instrumentation and the proliferation of global gravity data have been strongly fueled by various national defense needs. Today, there are two commercially available gravity gradiometers: the FTG by Bell Aerospace (now Lockheed Martin) and the Falcon by BHP Billiton. Both are a direct result of gravity gradiometry developments by the U. S. Navy. The FTG is used for land, marine, submarine, and airborne surveys, and the Falcon is used for airborne surveys only. In addition, Stanford University, the University of Western Australia, and ArkEx are each designing their own new airborne gravity gradiometer systems.

With the development of intercontinental ballistic missiles (ICBMs) early in the Cold War, a need arose for gravity mapping around all launch sites to correct a missile's flight path for perturbing gravitational effects resulting from local mass differences. With the advent of missile-launch-capable submarines, instruments were needed to collect detailed high-resolution gravity data on board submarines to map underwater missile launch sites. Although various gravity instruments had been used on board submarines since 1929 (Meinesz, 1929), they were inadequate for the Navy's requirements. To meet this need, the Navy developed a modern gravity gradiometer. In the late 1960s, Bell Aerospace (now Lockheed Martin), Hughes Aircraft, and MIT each began developing a classified gravity gradiometer for use on Navy submarines. The U. S. Navy chose to develop and deploy the Bell gravity gradiometer, known as the Full Tensor Gradient System, or FTG. The U. S. government dropped the development of the MIT instrument, but the Hughes Aircraft instrument, known as the Forward Gravity Gradiometer (named after its inventor, Robert L. Forward, a well-known gravity physicist and celebrated science-fiction author), continued its development under the auspices of the National Security Agency. After many years, the work on the Forward gradiometer was also discontinued.

The FTG system uses three small-diameter gravity gradient instruments (GGIs) mounted on an inertial stabilized platform. Each GGI contains four gravity accelerometers mounted on a rotating disk in a symmetric arrangement such that each of the individual accelerometer input axes are in the plane of the rotating disk, parallel to the circumference

of the disk and separated by 90°. The individual accelerometers consist of a proof mass on a pendulum-like suspension that is sensed by two capacitive pick-off rings located on either side of the mass. The signal generated by the pick-off system is amplified and converted to a current that forces the proof mass into a null position. The current is proportional to the acceleration. Vehicle accelerations are eliminated by frequency separation, where the gradient measurement is modulated at twice the disk-rotation frequency (0.25 Hz), leading to a forced harmonic oscillation. Any acceleration from a slight imbalance of opposing pairs of accelerometers is modulated by the rotation frequency. This permits each opposing pair of accelerometers to be balanced precisely and continuously. Six gravity gradient components are measured and referenced to three different coordinate frames. From these six components, five independent components can be reconstructed in a standard geographic reference frame. The remaining components of the gravity gradient tensor are constructed from Laplace's equation and the symmetry of the tensor. [For a review of the FTG sensor design, see Jekeli (1988) or Torge (1989).]

Although FTGs were initially intended for mapping underwater launch sites, submarines collected gravity data the entire time they were at sea. As submarine captains gained experience, they started to use underwater gravity as a navigational aid. The FTG data provided highly accurate mapping of seamounts and other sources of ocean-floor relief. The FTG, a very large instrument, was not portable but fit well into large nuclear submarines. In the mid-1980s, the U. S. Air Force began operating the FTG in a large van for land measurements. Later, the van was loaded onto a C130 aircraft for airborne measurements (Eckhardt, 1986).

In the mid-1990s, after the Cold War, both the Bell and the Forward instruments were declassified. In 1994, as a consequence of the downsizing of the U. S. missile submarine fleet, the U. S. government allowed both instruments to become commercialized to maintain the technology for future use. Bell Geospace acquired commercial rights to the FTG for marine surveying and immediately began acquiring marine data in the Gulf of Mexico for the hydrocarbon industry. At the same time, Lockheed Martin began to reengineer the FTG design to fit into a more portable platform, and by 2002, the FTG was deployed on fixed-wing airborne platforms. The FTG has also been used for land surveys over oil fields that are in secondary and tertiary recovery (DiFrancesco and Talwani, 2002).

Meanwhile, BHP Billiton, in agreement with Lockheed Martin, developed the Falcon system (Lee, 2001) for operation in small surveying aircraft aimed at shallow targets of interest to mineral exploration (see Case History). The Falcon, which collected its first airborne data in 1997, uses a single, large-diameter GGI with its axis of rotation close to vertical. The GGI is kept referenced to geographic coordinates so that the Falcon measures the differential curvature components of the gravity gradient tensor. The data may be transformed to the vertical gravitational acceleration, its vertical gradient, or any of the other components of the gravity gradient tensor by Fourier transform or equivalent source techniques.

The tremendous advantage that airborne gradiometry systems provide over conventional land/marine/airborne gravity systems is in their noise-reduction capabilities, speed of acquisition, and accuracy. The gradiometer design is relatively insensitive to aircraft accelerations, and with modern GPS

technology, it can be flown on very closely spaced survey lines. With appropriate processing, the gradiometer's sensitivity can be as fine as 3–8 EU and can resolve wavelengths of 300–1000 m. As the signal-to-noise ratio of gradiometer data acquisition and processing improves, there will be greater use of this technology, especially in remote regions where no prior conventional exploration has occurred.

### DATA ACQUISITION

The 20th century witnessed a tremendous expansion in both the science and the applications of gravity exploration, as demonstrated by the proliferation of the number of gravity stations. In 1900, there were only about 2000 gravity stations worldwide, all representing pendulum measurements. Beginning in the early 1930s, with the development of the torsion balance and then spring-gravity sensors, gravity data collection became much easier with improved resolution, which led to new applications in the mining, petroleum, civil engineering, military, and academic sectors. Early successes then fueled the development of new gravity instrument configurations such as marine, submarine, ocean-bottom, borehole, and airborne gravity instruments, which in turn inspired even more new applications of gravity techniques in those various sectors.

#### Land operations

As the number of torsion-balance crews began to dwindle in the 1940s, they were replaced largely by gravimeter crews, whose production in stations per day enjoyed a marked increase (LaFehr, 1980). In the last seven decades, more than 10 million stations have been acquired over nearly all of the earth's landmasses. Gravity operations have been conducted on polar ice, in jungles (where many stations have been located on tree stumps cut by chain saws), in marshes (on extended tripods), in very rugged topography such as the Overthrust Belt, and, of course, in hundreds of valleys from the Basin and Range Province of Nevada to the Amazon basin in South America and from the East African Rift Valley to the Pau Valley in France. In mining applications, there are numerous surveys in extremely rough topography. Without the resilience of these all-important field crews, we would not have a paper to write.

Gravimeter accuracy generally is not the limiting factor in producing meaningful interpretations of the final reduced anomalies. Errors resulting from position determination (especially elevations), terrain corrections, and geologic noise require the utmost care and usually more expense in the surveying component of field-crew operations.

Once high-quality gravity data are acquired, they do not become obsolete. The large volume of field activity, especially in the middle decades of the 20th century, has produced thousands of surveys now archived. The archived data are still of considerable value to explorationists as new techniques of interpretation, including integration with seismic and other geophysical and geological data, have evolved. The gravity method continues to be a small yet vital component of the geophysical exploration industry.

#### Underwater operations

Acquiring gravity data on the seafloor and lake bottoms was a natural extension of land operations and a major compo-

nent of gravity exploration budgets in the middle of the 20th century. At first, land meters and an operator were lowered in diving bells at stationary points in the water. Operations were conducted at night because positions were acquired by triangulating on light sources set up at separate points on the shoreline. These early efforts were soon replaced by remotely operated instruments and radio navigation systems.

Although the accuracy of underwater gravity measurements can approach that of land gravity systems, errors in the position of the meter location and in terrain corrections resulting from bathymetry limited the accuracy. Moreover, the high cost of underwater gravity acquisition and the recently improved navigational accuracies of marine gravity data have rendered underwater operations nearly extinct.

#### Sea-surface operations

While the history of dynamic gravity instrumentation explains in large measure the amazing success of this discipline, the evolution in field operations played a major and complementary role. The oceanographic research institutes have operated marine gravimeters since the 1950s. In 1962, Carl Bowin of Woods Hole Oceanographic Institution deployed the first marine gravity system with an automated digital acquisition system. In oil and gas exploration, the turning point in terms of prospect scale surveys came in 1965 in the first field test of the then new stabilized-platform L&R instrument (LaFehr and Nettleton, 1967). Even working on a very small vessel with the inferior (by today's standards) yet all-important positioning data and the need to understand and correct for directionally and sea-state-dependent cross-coupling effects, operators were able to produce exploration-quality results. The earlier L&R instruments swung freely in gimbals, and did not require cross-coupling corrections. Because the instrument was mounted on a stabilized platform, an attendant interaction between the vertical and horizontal accelerations produced unwanted motion effects, coined by LaCoste as cross-coupling. This effect and its correction were significant on all subsequent LaCoste meters until the advent of the straight-line meter (see History of Gravity Instrumentation).

Surface-ship surveys evolved from collecting only gravity and magnetic data surly on small ships in the mid-1960s to the massive 3D seismic vessels of today. In the 1960s and early 1970s, operating separately from seismic surveys was preferable because the gravity company controlled the operation: running under autopilot, with fewer course adjustments, reduced the higher frequency Eötvös effects and produced better-quality data than the data obtained during the more frequent course adjustments, typical of seismic surveys. It was obvious from the early days that dynamic gravity was limited by the accuracy of navigation data, not by the gravity sensor. In the late 1980s and 1990s, as GPS positioning became common, all of this changed.

In any case, marine gravity operations were largely dictated by economics. Almost all marine systems were owned and operated by seismic companies, and the acquisition of gravity data often did not receive the attention and priority required for high quality. Data quality varied widely from survey to survey. The pendulum shifted back to the gravity companies in the 1990s as the seismic companies divested their interests in

owning and operating gravity equipment. To the surprise of many, a new era of very high-quality surface-ship gravity data was ushered in by the very technology that had been thought to put gravity out of business: the closely spaced traverses of 3D seismic operations. Better determination of the Eötvös effects through improved GPS acquisition and processing; more stable platforms on the new, very large ships; and more comprehensive data reduction required by the very large data sets have led to better definition, in both wavelength and amplitude, of gravity anomalies acquired by surface ships than those obtained from underwater surveys. The definition of submilligal anomalies over subkilometer wavelengths became a reality.

### Airborne operations

In reviewing the history of dynamic gravity, it may be well to recall the initial skepticism endured by early advocates of both marine and airborne operations. Even one of the most prominent pioneers of gravity exploration technology, L. L. Nettleton, commented in the early 1960s that it was impossible to obtain exploration-quality data in moving environments. He reasoned that accelerations caused by sensor motion are mathematically indistinguishable from accelerations caused by subsurface density contrasts. (Of course, he had no way of knowing the impact GPS technology would have in identifying and removing motional effects.) Another prominent pioneer, Sigmund Hammer, held similar views until he was introduced to airborne gravity data flown over a large, shallow salt dome in the Gulf of Mexico. He was so excited by the potential of the method that he named his resulting paper "Airborne gravity is here," which generated intense and clamorous discussions (Hammer, 1983).

The important changes in marine gravity brought about by modern GPS acquisition and processing also revolutionized airborne operations. The high damping constant gives the L&R meter sensor a time constant of 0.4 ms (LaCoste, 1967). In the early 1970s, the highly filtered output of the gravimeter was sampled and recorded at 1-min intervals. Sometime around 1980, better digital recording and the desire to fine-tune cross-coupling corrections led to 10-s sampling, which was the standard until the early 1990s. Improved control electronics have helped to optimize the inherent sensitivity of gravity sensors, and GPS has provided accurate corrections for ship and airplane motion. At present, 1-Hz sampling is common for marine gravity acquisition, and 10-Hz sampling is common for airborne gravity.

GPS has provided the means to measure boat and aircraft velocity changes very accurately. This increased accuracy has led to faster reading of the gravimeter, more accurate corrections, less filtering, and minimized signal distortion as a result of filtering.

### Borehole gravity

The acquisition of gravity data in boreholes was discussed as early as 1950 when Neal Smith (1950) suggested that sampling large volumes of rock could improve rock density information. Hammer (1950) reported on the determination of density by underground gravity measurements. Although a considerable amount of effort in time and money was expended in the

early development of downhole measurements (Howell et al., 1966), this activity did not become a viable commercial enterprise until the advent of the L&R instrument in the 1960s and 1970s. During this era, data acquired by the U. S. Geological Survey (McCulloh, 1965) and Amoco Corp. (Bradley, 1974) confirmed the assessment previously made by Smith and resulted in L&R designing and building a new tool with dimensions and specifications more suitable for oil and gas exploration and exploitation.

In a BHGM survey, the average formation density is determined from  $\Delta g = 4\pi\rho G\Delta z$ , where  $\Delta z$  is the height difference between two points on the profile,  $\Delta g$  is the gravity difference between those two points,  $G$  is the universal gravitational constant, and  $\rho$  is the average formation density between those two points. The BHGM is the only logging tool capable of directly measuring average density at tens of meters from a well, and it is the only logging tool that can reliably obtain bulk density through casing. Because the BHGM is the only density logging tool that samples a large volume of formation to first order, it is not affected by near-borehole effects such as drilling mud, fluid invasion, formation damage, and casing or cement inhomogeneities.

Since 1970, about 1100 wells have been logged with the L&R instrument, but the prediction that borehole gravity use would increase (LaFehr, 1980) has not yet been borne out, primarily because the physical limitations of the BHGM have yet to be overcome. The difficulty lies in improving the limits of temperature, hole size, and deviation in such a way as to increase the applicability of the tool.

BHGMs have been used in exploration, formation evaluation, early and mature field development, enhanced oil recovery, and structural delineation (Chapin and Ander, 1999a,b). In particular, oil companies have used BHGMs in multiyear, time-lapse oil production monitoring (Schultz, 1989; Popta et al., 1990). The BHGM is also an outstanding tool in exploration for bypassed oil and gas, reliably indicating deposits previously overlooked. In addition, it has played a role in the study of possible sites for the burial of nuclear waste and has yielded interesting confirmation of the use of normal free-air correction (LaFehr and Chan, 1986).

### Satellite-derived gravity techniques

The modern era of satellite radar altimetry, beginning with Seasat in 1978, ushered in a golden age for imaging and mapping the global marine geoid and its first vertical derivative, the marine free-air gravity field. The advent of a public-domain global marine gravity database with uniform coverage and measurement quality (Sandwell and Smith, 1997, 2001) provided a significant improvement in our understanding of plate tectonics. This database represents the first detailed and continuously sampled view of marine gravity features throughout the world's oceans, enabling consistent mapping of large-scale structural features over their entire spatial extent. Understanding of the marine free-air gravity field continues to improve as additional radar altimeter data are acquired by new generations of satellites. The current CHAMP mission directly measures the global terrestrial and marine gravity fields at an altitude of 400 km (Reigber et al., 1996). This direct measurement provides important information on the long-wavelength components of the global gravity field.

The GRACE and GOCE satellites are also designed for direct measurement of the global gravity field (Tapley et al., 1996; Tapley and Kim, 2001).

The Seasat mission, launched by NASA in 1978, was equipped with oceanographic monitoring sensors and a radar altimeter. The altimeter was designed to measure sea-surface topography in an attempt to document the relief caused by water displacement from either large-scale ocean currents (e.g., the Gulf Stream) or water mounding caused by local gravity anomalies within the earth's crust and upper mantle. Earlier missions [Skylab (1973) and GOES-3 (1975–1978)] provided proof of concept that radar altimetry could image ocean surface relief. The three-month Seasat mission provided the first complete imaging of sea-surface relief and completely changed earth scientists' understanding of tectonic processes at work, from the continental margins to abyssal plains and from midoceanic ridges to subduction zones.

Sea-surface topography can be used to compute the marine gravity field (Sandwell and Smith, 1997; Hwang et al., 1998). The approach is based on the ocean's ability to deform and flow in the presence of an anomalous mass excess or deficiency. The ocean surface, as a liquid, is capable of responding dynamically to lateral density contrasts within the solid earth: denser columns of rock will amass more seawater above them. The mean sea surface is the geoid, the equipotential surface defined throughout the world's oceans (and continuing onshore). Prior to the Seasat mission, geodesists understood that geoidal relief should be in the tens to hundreds of meters (Rapp and Yi, 1997). With the Seasat results, however, geodesists and geophysicists could finally document the geoid's relief, wavelength, and anomaly character (Haxby et al., 1983; Stewart, 1985). Once the marine geoid could be mapped, deriving the vertical component of the gravity field became a simple derivative computation because the geoid is its integral.

Fueled by the success of Seasat and the insight it provided the geologic community, new missions were planned and successfully launched by NASA and the European Space Agency (ESA). The Topex/Poseidon, Geosat, ERS1, and ERS2 satellites provided improved resolution and accuracy in mapping sea-surface topography. Continued research into better defining the gravity field and its implications for the earth's tectonic history have been conducted by Sandwell and Smith (1997), Cazenave et al. (1996), Cazenave and Royer (2001), and others.

For more than 15 years, the exploration community has made tremendous use of the global marine satellite-derived gravity field. Our ability to image structural components within the continental margins worldwide has produced countless important new leads offshore. Despite the relatively long-wavelength resolution (7–30 km) of the satellite-derived gravity field (Yale et al., 1998), its ubiquitous coverage and consistent quality are invaluable (Figure 1).

Follow-up missions have been proposed (Sandwell et al., 2003) for flying higher-

resolution and more precise altimeters with more closely spaced orbital paths. These would further enhance the resolution of the derived gravity field, allowing 5–10-km anomaly wavelength resolution with 2–5-mGal accuracy. Although the gravity anomalies from individual salt domes may never be imaged from satellite-based radar altimeters, individual basins and their structural complexity have already been mapped with greater accuracy.

## DATA REDUCTION AND PROCESSING

Gravity data reduction is a process that begins with a gravimeter reading at a known location (the gravity station) and ends with one or more gravity anomaly values at the same location. The gravity anomaly values are derived through corrections to remove various effects of a defined earth model. The basic reduction of gravity data has not changed substantially during the past 75 years; what has changed is the speed of the computations. In the late 1950s, Heiskanen and Meinesz (1958) maintained that barely more than one rough-mountain station a day could be reduced by one computer. In 1958, a "computer" was a person who calculated data. Today, with digital terrain data and electronic computers, full-terrain and isostatic corrections can be calculated in seconds.

Corrections leading to the complete Bouguer anomaly are relatively independent of the geology and are called the standard reduction by LaFehr (1991a). The isostatic correction, on the other hand, requires selecting a geologic geodynamic model for isostatic compensation. Additional processing options such as the specification of a nonstandard reduction density to remove residual terrain effects (Nettleton, 1939) or terrain corrections using variable densities (Vajk, 1956; Grant and Elsharty, 1962) stray even farther into the realm of data interpretation.

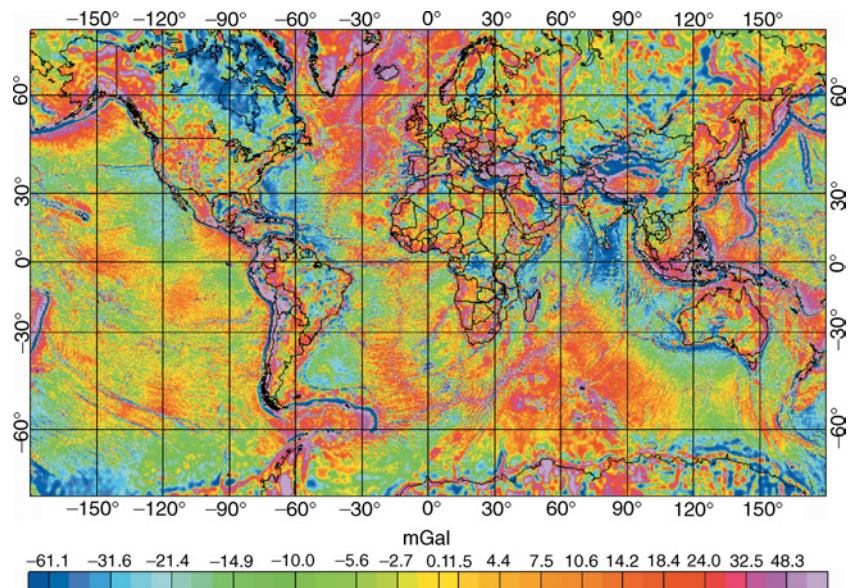


Figure 1. Satellite-derived marine free-air gravity field, merged with terrestrial gravity field, published by Sandwell and Smith (2001), courtesy of the NOAA-NGDC.

Contrary to the approach used in many standard textbooks, it is best to think of gravity corrections as being applied to the theoretical gravity value calculated on the reference ellipsoid to bring the theoretical value up to the elevation of the measurement before it is subtracted from the measured value. This way, the gravity anomaly value is defined at the measurement location rather than on the ellipsoid or geoid (Hayford and Bowie, 1912; LaFehr, 1991a; Chapin, 1996). The geodetic reference system used to determine the calculated value of the ellipsoid or geoid is updated occasionally. Before 1967, an International Ellipsoid (adopted in 1924) and an International Gravity Formula (adopted in 1930) were used. Today the Geodetic Reference System of 1967 (International Association of Geodesy, 1971) and the International Gravity Standardization Net of 1971 (Morelli, 1974) are commonly used. The emerging standard is based on the Geodetic Reference System of 1980 (Moritz, 1980).

Today, as in the past, Gravity measurement locations are usually referenced to the sea-level surface or local geoid as determined by station elevation. Theoretical gravity, which ranges from about 978 000 mGal at the equator to 983 000 mGal at the poles, is calculated on the geoid before corrections are applied. In the future, GPS elevation measurements, which are referenced to the ellipsoid rather than the geoid, will increase the likelihood that the ellipsoid will supplant the geoid as the standard reference surface. By using the ellipsoid and GPS locations, gravity surveys can be conducted in areas where traditional geoid elevations are unavailable or unreliable.

### Standard data reduction

The reduction of gravity data proceeds from simple meter corrections to corrections that rely on increasingly sophisticated earth models. The corrections and their application are described adequately in most basic geophysical textbooks. However, important details of the reduction equations continue to be refined and debated (LaFehr, 1991a,b, 1998; Chapin, 1996; Talwani, 1998). In addition, recent use of GPS technology has increased the confusion over use of the ellipsoid versus the geoid in data reduction (Li and Götze, 2001). These equations have been documented and standardized by the Standards/Format Working Group of the North American Gravity Database Committee (Hinze et al., 2005).

The gravity observation at a station requires knowledge of the measurement time, the meter constant, the drift rate and characteristics, and the absolute gravity value at a base station when relative gravimeters are used. The basic data reduction requires knowledge of the station latitude to compute the theoretical gravity on the ellipsoid or at sea level. The free-air correction requires knowledge of the standard gradient of gravity in addition to the elevation. The standard gradient of gravity has long been considered as 0.3086 mGal/m, but improved computational abilities may allow additional precision (Hildenbrand et al., 2002; Hinze et al., 2005). The free-air correction reduces the theoretical gravity by 2731 mGal at the summit of Mt. Everest and increases it by 3368 mGal in the Challenger Deep. Free-air anomalies are preferred for modeling density structure of the full crust, from the topography to the Moho. They are generally used for construction of grav-

ity anomaly maps offshore. Free-air gravity anomalies useful for regional studies in offshore areas can be generated directly from satellite altimetry data (Sandwell and Smith, 1997; see also Satellite-Derived Gravity Techniques).

The free-air anomaly can be, but rarely is, refined by applying a correction for the mass of the atmosphere above the station. This mass is included in the calculated theoretical gravity, but under a spherical approximation, the correction only applies to stations unrealistically located above the atmospheric mass (Ecker and Mittermayer, 1969; Moritz, 1980; Wenzel, 1985; Hildenbrand et al., 2002; Hinze et al., 2005). The atmospheric correction reduces the theoretical gravity by 0.87 mGal at sea level and by 0.28 mGal at the summit of Mt. Everest.

The simple (or incomplete or Bullard A) Bouguer correction is added to the theoretical gravity at the measurement location. The correction represents the effect of a uniform slab having a thickness equal to the station elevation and a given density (typically 2670 kg/m<sup>3</sup>). The correction ranges from 991 mGal at the summit of Mount Everest to -764 mGal in the Challenger Deep. Simple Bouguer anomalies have all primary elevation effects removed and therefore are popular for the construction of gravity anomaly maps on land.

The Bouguer slab is only a first approximation to a spherical cap having a thickness equal to the station elevation and the chosen density. The curvature (Bullard B) correction, often ignored in textbooks, adds the remaining terms for the gravity effect of the spherical cap to the theoretical gravity. This amounts to about 0.2 mGal. The arc-length radius of 166.7 km used for the spherical cap is based on minimizing the contribution of the curvature correction over a common range of latitudes. The publication of a new version for the curvature correction (LaFehr, 1991b) has brought renewed attention to this second step in Bouguer reduction.

A terrain-corrected Bouguer anomaly is called a complete Bouguer anomaly, where the terrain represents the deviations from the uniform slab of the simple Bouguer correction or the spherical cap of the curvature correction. An excess of mass resulting from terrain above the station reduces the observed gravity, as does a deficiency of mass resulting from terrain below the station. An exception occurs when airborne gravity is being reduced to the level of the ground surface (as opposed to the flight surface). In this case, terrain corrections can have either sign in rough topography.

Before the availability of digital terrain data, terrain corrections were calculated graphically by laying a template resembling a dartboard over a topographic map, averaging elevations within segments of annular zones about the gravity station, and using a table to determine the terrain correction (Hammer, 1939). Inner-zone terrain corrections are still done this way, although reflectorless laser, range-finding systems are becoming more popular (Lyman et al., 1997). Bott (1959) and Kane (1960, 1962) were the first to use digital terrain data for terrain corrections. Today, Plouff's (1977) computer algorithm is the standard.

In rough topography, the magnitude of terrain corrections can exceed 30 mGal, and accuracy is limited by the ability to estimate inner-zone terrain corrections precisely in the field and by the quality of the digital elevation model. Generally, a single density is used for terrain corrections. Methods using

variable surface density models have been proposed by Vajk (1956) and Grant and Elsharty (1962).

### Additional corrections

Even after topographic correction, the Bouguer anomaly contains large negative anomalies over mountain ranges, indicating the need for additional corrections such as isostatic and decompensation, which require some knowledge or assumptions about geologic models. Isostatic corrections are intended to remove the effect of masses in the deep crust or mantle that isostatically compensate for topographic loads at the surface. Under an Airy model (Airy, 1855), the compensation is accomplished by crustal roots under the high topography, which intrude into the higher-density material of the mantle to provide buoyancy for the high elevations. Over oceans, the situation is reversed. The Airy isostatic correction assumes that the Moho is like a scaled mirror image of the smoothed topography, that the density contrast across the Moho is a constant, and that the thickness of the crust at the shoreline is a known constant. Scaling is determined by the density contrast and by the fact that the mass deficiency at depth must equal the mass excess of the topography for the topography to be in isostatic equilibrium. Isostatic corrections can also be made for the Pratt model, in which the average densities of the crust and upper mantle vary laterally above a fixed compensation depth. Isostatic corrections are relatively insensitive to the choice of model and to the exact parameter values used (Simpson et al., 1986). The isostatic residual gravity anomaly is preferred for displaying and modeling the density structure of the middle and upper crust.

Like terrain corrections, early isostatic corrections were accomplished by means of templates and tables. Some implementations of isostatic corrections using digital computers and digital terrain data include Jachens and Roberts (1981), Sprenke and Kanasevich (1982), and Simpson et al. (1983). The latter algorithm was used to produce an isostatic residual gravity anomaly map for the conterminous United States (Simpson et al., 1986).

The isostatic correction is designed to remove the gravity effect of crustal roots produced by topographic highs or lows but not the effect of crustal roots derived from regions of increased crustal density without topographic expression. The decompensation correction (Zorin et al., 1985; Cordell et al., 1991) is an attempt to remedy this. It is calculated as an upward-continued isostatic residual anomaly, taken to represent the anomalies produced in the deeper crust and upper mantle. The correction is subtracted from the isostatic residual anomaly to produce the decompensation gravity anomaly. The decompensation correction has been applied to isostatic residual gravity anomaly data of Western Australia to compare the oceanic crust with the shallow continental crust (Lockwood, 2004).

### Gridding

Once gravity data are reduced to the form of gravity anomalies, the next step usually involves gridding the data to produce a map, apply filters, or facilitate 3D interpretation. Because gravity data can be collected along profiles such as ship tracks or roads, as well as in scattered points, the standard gridding

algorithm is minimum curvature (Briggs, 1974). For situations such as marine surveys with parallel ship tracks or airborne surveys, the gridding algorithm may be required to reduce cross-track aliasing. Here, an algorithm with some degree of trend enhancement such as anisotropic kriging (Hansen, 1993) or gradient-enhanced minimum curvature (O'Connell et al., 2005) could be used.

## DATA FILTERING AND ENHANCEMENT

A common first step before interpretation is to render the observed data into a different form by filtering or enhancement techniques. The goal may be to support subsequent application of other techniques, facilitate comparison with other data sets, enhance gravity anomalies of interest, and/or gain some preliminary information on source location or density contrast. Most filter and interpretation techniques apply to both gravity and magnetic data. As such, it is common to reference a paper describing a technique for filtering magnetic data when processing gravity data and vice versa.

### Regional-residual separation

Anomalies of interest are commonly superposed on a regional field caused by sources larger than the scale of study or too deep to be of interest. In this situation, it is important to perform a regional-residual separation, a crucial first step in data interpretation. Historically, this problem has been approached either by using a simple graphical approach (manually selecting data points to represent a smooth regional field) or by using various mathematical tools to obtain the regional field. Many of the historical methods are still in common use today.

The graphical approach initially was limited to analyzing profile data and, to a lesser extent, gridded data. The earliest nongraphic approach used a regional field defined as the average of field values over a circle of a given radius, with the residual being the difference between the observed value at the center of the circle and this average (Griffin, 1949). Henderson and Zietz (1949) and Roy (1958) showed that such averaging was equivalent to calculating the second vertical derivative except for a constant factor. Agoes (1951) proposed using a least-squares fit to data to determine the regional field, an approach criticized by Skeels (1967), since the anomalies themselves will affect somewhat the determined regional. Hammer's (1963) paper on stripping proposed that the effect of shallow sources could be removed through gravity modeling. Zurflueh (1967) proposed using 2D linear-wavelength filtering with filters of different cutoff wavelengths to solve the problem. The method was further expanded by Agarwal and Kanasevich (1971), who also used a crosscorrelation function to obtain trend directions from magnetic data. Syberg (1972a) described a method using a matched filter for separating the residual field from the regional field. A method based on frequency-domain Wiener filtering was proposed by Pawlowski and Hansen (1990).

Spector and Grant (1970) analyzed the shape of power spectra calculated from observed data. Clear breaks between low- and high-frequency components of the spectrum were used to design either band-pass or matched filters. Guspi and Introcaso (2000) used the spectrum of observed data and looked

for clear breaks between the low- and high-frequency components of the spectrum to separate the regional and residual fields.

Matched filters and Wiener filters have much in common with other linear band-pass filters but have the distinct advantage of being optimal for a class of geologic models. Based on experience, it seems that significantly better results can be obtained by using appropriate statistical geological models rather than by attempting to adjust band-pass filter parameters manually.

The existence of so many techniques for regional-residual separation demonstrates that unresolved problems still exist in this area. There is no single right answer for how to highlight one's target of interest.

### Upward-downward continuation

In most cases, gravity anomaly data are interpreted on (or near) the original observation surface. In some situations, however, it is useful to move (or continue) the data to another surface for interpretation or for comparison with another data set. One example might involve upward-continuing land or sea-surface gravity data for comparison with airborne or satellite gravity or magnetic data.

Gravity data measured on a given plane can be transformed mathematically to data measured at a higher or lower elevation, thus either attenuating or emphasizing shorter-wavelength anomalies (Kellogg, 1953). These analytic continuations lead to convolution integrals that can be solved either in the space or the frequency domain. The earliest attempts were done in the space domain by deriving a set of weights that, when convolved with field data, yielded approximately the desired transform (Peters, 1949; Henderson, 1960; Byerly, 1965). Fuller (1967) developed a rigorous approach to determine the required weights and to analyze their performance. The space-domain operators were soon replaced by frequency-domain operators. Dean (1958) was the first to recognize the utility of using Fourier transform techniques in performing analytic continuations. Bhattacharyya (1965), Mesko (1965), and Clarke (1969) contributed to the understanding of such transforms, which now are carried out routinely. Whereas upward continuation is a very stable operation, the opposite is true for downward continuation, where special techniques, including filter response tapering and regularization, must be applied to control noise.

Standard Fourier filtering techniques only permit analytic continuation from one level surface to another. To overcome this limitation, Syberg (1972b) and Hansen and Miyazaki (1984) extended the potential field theory to allow continuation between arbitrary surfaces, and Parker and Klitgord (1972) used a Schwarz-Christoffel transformation to upward-continue uneven profile data. Cordell (1985) introduced the chessboard technique, which calculates the field at successively higher elevations followed by a vertical interpolation between various strata, and an analytic continuation based on a Taylor-series expansion. An alternative approach uses an equivalent-source gridding routine (Cordell, 1992; Mendonça and Silva, 1994, 1995) to determine a buried equivalent mass distribution that produces the observed gravity anomaly and then uses the obtained equivalent masses to calculate the gravity anomaly on the topographic grid. An equivalent-point

source inversion method for spherical earth and gravity analysis was proposed by von Frese et al. (1981) to facilitate geologic interpretation of satellite elevation potential-Field data. An equivalent source method in wave number domain was proposed by Xia et al. (1993). For faster convergence and better representation of shorter wavelengths, Phillips (1996) extended this method into a hybrid technique using the approach of Cordell (1992).

### Derivative-based filters

First and second vertical derivatives are commonly computed from gravity data to emphasize short-wavelength anomalies resulting from shallow sources. They can be calculated in both the space and frequency domains using standard operators. Unfortunately, these operators amplify the higher frequency noise, so special tapering of the frequency response is usually required to control noise. A stable calculation of the first vertical derivative was proposed by Nabighian (1984) using 3D Hilbert transforms in the  $x$ - and  $y$ -directions.

Horizontal derivatives, which can easily be computed in the space domain, are now the most common method for detecting target edges. Cordell (1979) first demonstrated that peaks in the magnitude of the total horizontal gradient of gravity data (square root of the sum of squares of the  $x$ - and  $y$ -derivatives) could be used to map near-vertical boundaries of contrasting densities, such as faults and geologic contacts. The method became more widely used following subsequent papers discussing various aspects of the method and showing its utility (Cordell and Grauch, 1982, 1985; Blakely and Simpson, 1986; Grauch and Cordell, 1987; Sharpton et al., 1987). In map form, the magnitude of the horizontal gradient can be gridded to display maximum ridges situated approximately over the near-vertical lithological contacts and faults.

Blakely and Simpson (1986) developed a useful method for gridded data, automatically locating and plotting the maxima of the horizontal gradient magnitude. A method by Pearson (2001) finds breaks in the horizontal derivative direction by applying a moving-window artificial intelligence operator. A similar technique is skeletonization (Eaton and Vasudevan, 2004); this produces both an image and a database of each lineament element, which can be sorted and decimated by length or azimuth criteria. Thurston and Brown (1994) have developed convolution operators for controlling the frequency content of the horizontal derivatives and, thus, of the resulting edges. Cooper and Cowan (2003) introduced the combination of visualization techniques and fractional horizontal gradients to more precisely highlight subtle features of interest.

The tilt angle, introduced by Miller and Singh (1994), is the ratio of the first vertical derivative to the horizontal gradient. The tilt angle enhances subtle and prominent features evenly, so the edges mapped by the tilt derivative are not biased toward the largest gradient magnitudes. Grauch and Johnston (2002) address the same problem by computing horizontal gradients within moving windows to focus on regional versus local gradients.

Another form of filter that can be used to highlight faults is the Goussev filter, which is the scalar difference between the total gradient and the horizontal gradient (Goussev et al., 2003). This filter, in combination with a depth separation filter (Jacobsen, 1987), provides a different perspective than other

filters and helps discriminate between contacts and simple offset faults. Wrench faults show up particularly well as breaks in the linear patterns of a Goussev filter.

Although less common in gravity methods than in magnetic techniques, Euler and Werner deconvolution edge and depth-estimation techniques can help define the lateral location and depth of isolated faults and boundaries from gravity data. Complex geology with overlapping anomalies arising from different depths can, however, limit the effectiveness of deconvolution fault-detection results.

Display techniques can also be used to enhance anomalies or gradients from linear boundaries such as faults. Although fault expressions are visible on filtered gravity profiles, their trends can be much easier to trace on shaded relief images. Expressions of faults can best be seen when the synthetic sun angle is perpendicular to the fault strike. Since a given sun direction highlights features that strike perpendicular to it, it is important to generate enough images with varying sun angles to illuminate all azimuths of lineament/fault trends. Today, many imaging algorithms allow real-time variation of sun angle and 3D perspective, permitting an interpreter to choose quickly the images that best reflect the underlying geology.

### Analytic signal

The analytic signal, although extensively used in magnetics, is used little in gravity techniques, primarily because of the sparser nature of gravity data, which makes the calculation of derivatives less reliable. For magnetic profile data the horizontal and vertical derivatives fit naturally into the real and imaginary parts of a complex analytic signal (Nabighian, 1972, 1974, 1984; Craig, 1996). In two dimensions (Nabighian, 1972), the amplitude of the analytic signal is the same as the total gradient. In three dimensions, Roest et al. (1992) introduced the total gradient of magnetic data as an extension to the 2D case. The results obtained for magnetic data can be extended to gravity data if one uses as input the horizontal derivative of the gravity field. What is now commonly called the 3D analytic signal should correctly be called the total gradient.

### Matched filtering

If the spectrum of the expected signal is known, matched filtering can help locate the signal in a given data set. The matched filter has the same spectrum as the desired signal. In potential field methods, matched filtering primarily has been used to separate data into anomaly components representing different source depths. The method was first developed for use with magnetic data when Spector (1968) and Spector and Grant (1970) showed that logarithmic radial power spectra of aeromagnetic map data contain straight slope segments that can be interpreted as arising from statistical ensembles of sources or equivalent source layers at different depths. Spector (1968) applied matched filtering in both frequency and space domains. Syberg (1972a), who introduced the term *matched filter*, applied the technique to modeling azimuthal variations within each band pass. Ridsdill-Smith (1998a,b) developed wavelet-based matched filters, while Phillips (2001) generalized the Fourier approach of Syberg (1972a) to sources

at more than two depths and explained how matched Wiener filters could be used as an alternative to the more common amplitude filters.

An alternative to matched filters, based on differencing upward-continued fields, was developed by Jacobsen (1987). Cowan and Cowan (1993) reviewed separation filtering and compared results of Spector's matched filter, the Cordell filter, the Jacobsen filter, and a second vertical derivative filter on an aeromagnetic data set from Western Australia.

### Wavelets

The wavelet transform is emerging as an important processing technique in potential-field methods and has contributed significantly to the processing and inversion of both gravity and magnetic data. The concept of continuous wavelet transform was introduced initially in seismic data processing (Goupillaud et al., 1984), while a form of discrete wavelet transform has long been used in communication theory. These were unified through an explosion of theoretical developments in applied mathematics. Potential-field analysis — magnetic methods in particular — have benefited greatly from these developments.

Moreau et al. (1997) were the first to use continuous-wavelet transform to analyze potential-field data for simple monopole sources. In a seminal paper, Hornby et al. (1999) independently developed a similar theory and recast commonly used processing methods in potential fields in terms of continuous-wavelet transform. These wavelets are essentially different second-order derivatives of the potential produced by a point monopole source. Methods based on continuous-wavelet transform identify locations and boundaries of causative bodies by tracking the extrema of wavelet transforms. Marlet et al. (2001) applied a similar wavelet transform to gravity data to identify geologic boundaries.

A second approach is applied primarily for data processing that uses discrete-wavelet transforms based on compactly supported orthonormal wavelets. Chapin (1997) applied wavelet transform to the interpretation of gravity and magnetic profiles. Ridsdill-Smith and Dentith (1999) published a paper on processing aeromagnetic data, which generally is applicable to gravity data as well. Lyrio et al. (2004) improved upon the concept of wavelet denoising in signal processing and applied it to processing of gravity gradiometry data by first estimating the noise level in the wavelet domain and then removing the noise accordingly.

Finally, discrete-wavelet transforms were used as a means to improve numerical efficiency of conventional processing methods. Li and Oldenburg (1997, 2003) compressed the dense sensitivity matrix in 3D inversion to reduce both memory requirement and CPU time in large-scale 3D inverse problems. A similar approach has also been applied to the problem of upward continuation from uneven surfaces using equivalent sources (Li and Oldenburg, 1999).

## DATA INTERPRETATION

Ideally, the final outcome of data interpretation is a physical property map. A general solution for this problem is not available now, but some approximate solutions are used in various applications.

### Terracing

Terracing (Cordell and McCafferty, 1989) is an iterative filtering method that gradually increases the slopes of anomalies until they become vertical while simultaneously flattening the field between gradients. The resulting map is similar to a terraced landscape; hence, the name applied to this technique. When imaged as a color map and illuminated from above, a terraced map resembles a geologic map in which the color scheme reflects relative density contrasts. The terrace map can be further refined into a density map by iterative forward modeling and scaling of the terraced values.

### Density mapping

Several popular magnetic-anomaly interpretation techniques can easily be adapted to gravity data. Grant (1973) introduced a special form of inversion in which magnetic data are inverted in the frequency domain to provide the apparent magnetic susceptibility of a basement represented by a large number of infinite vertical prisms. The resulting maps provided a better geologic interpretation in the survey area. The method was later extended to the space domain by solving a large system of equations relating the observed data to magnetic sources in the ground (Bhattacharyya and Chan, 1977; Misener et al., 1984; Silva and Hohmann, 1984).

Another approach was taken by Keating (1992), who assumed an earth model consisting of right rectangular prisms of finite depth extent and used Walsh transforms to determine the density of each block. Granser et al. (1989) used the power spectrum of gravity data to separate it into long- and short-wavelength components and then applied an inverse density deconvolution filter to the short-wavelength components to obtain density values for the upper crust. Finally, as mentioned previously, the terracing method (Cordell and McCafferty, 1989) can be used for density determinations.

### GRAVITY FORWARD MODELING

Before the use of electronic computers gravity and magnetic anomalies were interpreted using characteristic curves calculated from simple models (Nettleton, 1942). The publication of Talwani et al.'s (1959) equations for computing gravity anomalies produced by 2D bodies of polygonal cross section provided the impetus for the first use of computers for gravity modeling. The 2D sources were later modified to have a finite strike length (Rasmussen and Pedersen, 1979; Cady, 1980). This led to publicly available computer programs for 2.5-D gravity modeling (Webring, 1985; Saltus and Blakely, 1983, 1993).

Three-dimensional density distributions initially were modeled by Talwani and Ewing (1960) using thin, horizontal, polygonal plates. Plouff (1975, 1976) showed that, in certain cases, the use of finite-thickness horizontal plates was a practical and preferable alternative. Right rectangular prisms (Nagy, 1966) and dipping prisms (Hjelt, 1974) remain popular for building complex density models, especially as inexpensive computers become faster. Barnett (1976) used triangular facets to construct 3D bodies of arbitrary shape and to compute their gravity anomalies, whereas Okabe (1979) used polygonal facets.

Parker (1972) was the first to use Fourier transforms to calculate 2D and 3D gravity anomalies from complexly layered models. Because the gravity anomaly is calculated on a flat observation surface above all sources, this approach is particularly well suited to modeling marine gravity data. Fourier methods can provide an alternative to spatial-domain approaches for modeling simple sources such as a point mass or a uniform sphere, a vertical line mass, a horizontal line mass, or a vertical ribbon mass (Blakely, 1995). Blakely (1995) also presented the theory and computer subroutines for computing gravity fields of simple bodies in the spatial domain, including a sphere, a horizontal cylinder, a right rectangular prism, a 2D body of polygonal cross section, and a horizontal layer.

Today, forward gravity modeling is often done using commercial software programs based on the theory and early software efforts mentioned above but incorporating inversion algorithms and sophisticated computer graphics. A relatively recent development in forward modeling is the concept of structural geophysics (Jessell et al., 1993; Jessell and Valenta, 1996; Jessell, 2001; Jessell and Fractal Geophysics, 2001), in which a layered-earth model having specified physical properties is subjected to a deformation history involving tilting, faulting, folding, intrusion, and erosion. The resulting gravity field is computed using deformed prisms based on the model of Hjelt (1974).

### GRAVITY INVERSE MODELING

Inversion is defined here as an automated numerical procedure that constructs a model of subsurface physical property (density) variations from measured data and any prior information independent of the measured data. Quantitative interpretation is then carried out by drawing geologic conclusions from the inverted models. A model is either parameterized to describe source geometry or is described by a distribution of a physical property such as density or magnetic susceptibility contrast. The development of inversion algorithms naturally followed these two directions. Bott (1960) first attempted to invert for basin depth from gravity data by adjusting the depth of vertical prisms through trial and error. Danes (1960) used a similar approach to determine the top of salt. Oldenburg (1974) adopted Parker's (1972) forward procedure in the Fourier domain to formulate an inversion algorithm for basin depth by applying formal inverse theory. A number of authors extended the approach to different density-depth functions or imposed various constraints on the basement relief (e.g., Pedersen, 1977; Chai and Hinze, 1988; Reamer and Ferguson, 1989; Guspi, 1992; Barbosa et al., 1997).

Recently, this general methodology has been used extensively in inversion for base of salt in oil and gas exploration (e.g., Jorgensen and Kisabeth, 2000; Nagihara and Hall, 2001; Cheng et al., 2003). A similar approach has been used to invert for the geometry of isolated causative bodies by representing them as polygonal bodies in two dimensions or polyhedral bodies in three dimensions (Pedersen, 1979; Moraes and Hansen, 2001) in which the vertices of the objects are recovered as the unknowns. Alternatively, one may invert for density contrast as a function of position in the subsurface. Green (1975) applied the Backus-Gilbert approach to invert 2D gravity data and guided the inversion by using reference

models and associated weights constructed from prior information. In a similar direction, Last and Kubik (1983) guided the inversion by minimizing the total volume of the causative body, and Guillen and Menichetti (1984) chose to minimize the inertia of the body with respect to the center of the body or an axis passing through it.

While these approaches are effective, they are limited to recovering only single bodies. Li and Oldenburg (1998) formulated a generalized 3D inversion of gravity data by using the Tikhonov regularization and a model objective function that measures the structural complexity of the model. A lower and upper bound are also imposed on the recovered density contrast to further stabilize the solution. A similar approach has been extended to the inversion of gravity gradient data (Li, 2001; Zhdanov et al., 2004). More recently, there have been efforts to combine the strengths of these two approaches. Krahenbuhl and Li (2002, 2004) formulated the base-of-salt inversion as a binary problem, and Zhang et al. (2004) took a similar approach for crustal studies. Interestingly, in the last approaches the genetic algorithm has been used as the basic solver. This is an area of growing interest, especially when refinement of inversion is desired with constraints based on prior information.

## GEOLOGIC INTERPRETATION

Observed gravity anomalies are direct indications of lateral contrasts in density between adjacent vertical columns of rock. These columns extend from the earth's terrestrial or sea surface to depths ranging from about 10 m to more than 100 km. The gravity surveying process measures the sum of all lateral density contrasts at all depths within this column of rock. Data filtering allows one to isolate portions of the gravity anomaly signal that are of exploration interest. These target signatures can then be interpreted together with ancillary geologic information to construct a constrained shallow-earth model.

### Density contrasts

Gravity signatures from relatively shallow-density-contrast sources have historically been used in both mineral and hydrocarbon exploration to identify important geologic targets for which there was a density contrast  $\Delta\rho$  at depth. Examples include ore bodies ( $+\Delta\rho$ ), salt domes within sediments salt domes ( $+$  or  $-\Delta$ ), depending on the surrounding sediments sulfur (complex  $\Delta\rho$  distribution), basin geometry ( $-\Delta\rho$ ), reefs ( $+$  or  $-\Delta\rho$ , depending on porosity and depth), carbonate leading edges of thrust sheets ( $+\Delta\rho$ ), faults (gradient lineaments, downthrown or footwall side indicated by lower gravity), anticlines and horst blocks ( $+\Delta\rho$ ), regional geology (complex  $\Delta\rho$  distribution and gradient lineaments), and kimberlite pipes ( $+$  or  $-\Delta\rho$ , depending on *country* rock and degree of weathering).

The wealth of density databases compiled over the years (Dobrin, 1976; Carmichael, 1984) is valuable for establishing standardized relationships of rock properties and gravity signatures. However, it is recommended that, whenever possible, one measure densities on relevant rock samples.

### Physical properties in boreholes

Hundreds of thousands of individual density determinations have been accumulated in thousands of wells around

the earth, generally at depths shallower than 5 km. Computed densities are often called bulk density or in-situ density (McCulloh, 1965; Robbins, 1981). McCulloh et al. (1968) explained in some detail the need for a variety of corrections (for example, hole rugosity, terrain, and nonlevel geologic effects) to justify the use of the term formation density.

LaFehr (1983) suggested the term *apparent density* to account for structural effects (a nonhorizontal, uniformly layered earth) at or near the well in a manner analogous to the use of the term *apparent velocity* when working with seismic refraction data or other apparent geophysical measurements. Thus, the apparent density is not the actual rock density, even if measurements are error free. An interesting result of potential-field theory is the Poisson jump phenomenon, in which borehole gravity measurements can yield the actual change in density across geologic boundaries because the difference between the bulk and apparent densities is the same on both sides of the boundary (for wells penetrating geologic boundaries at normal incidence). The Poisson jump has been observed in many different geologic settings. An example is the Mors salt dome in Denmark (LaFehr et al., 1983), in which laboratory-studied cores as well as surface seismic information helped to confirm the borehole gravity results.

The physical properties obtainable from borehole gravity surveys include density and porosity. The latter requires independent knowledge of matrix and fluid densities. Two general classes of applications can be addressed: (1) formation evaluation or, in the case of known reservoirs, reservoir characterization and (2) remote sensing. In the latter application, a rule of thumb for 2D geology is that the apparent-density anomaly caused by a remote density boundary is proportional to the angle subtended in the wellbore by the remote boundary. For 3D geologic structures symmetric about the wellbore, as approximated in some carbonate reef cases, the apparent-density anomaly is proportional to the sine of the subtended angle.

## DATA INTEGRATION AND PRESENTATION

The goal of the explorationist is to use knowledge derived from the gravity field to improve understanding of the local or regional geologic setting and, in turn, to better grasp the exploration potential of the area of interest. To minimize the nonuniqueness of this endeavor, constant and rigorous integration of gravity data with other geophysical and geological information is required in all interpretation projects. Two-dimensional and three-dimensional modeling software can now readily incorporate geologic information in the form of well-log densities, top-structure grids or horizons, locations of faults, and other geologic constraints. This flexibility allows the interpreter to establish end-member geometries and density contrasts for earth models that can (or cannot) satisfy the observed gravity signature. A complete modeling effort includes several models which demonstrate the range of geologically plausible models that fit the data. When modeling, one can choose to match the complete gravity signature or a residual component. If the residual is modeled, the earth model must be consistent with this signal, i.e., the same gravity effects must be removed from the earth model that were subtracted from the complete gravity signal.

The ability to visualize the different components of the gravity field has improved exponentially with the advent of low-cost, high-speed imaging software. Geologically constrained interpretation of gravity data requires the use of other information. Modern interpretation techniques make extensive use of 2D and 3D depth-converted seismic data, density-log information, electromagnetic information, elevation models, and satellite imagery. The K-2 case history (following) illustrates the use of gravity in combination with seismic data to image a structure not readily interpretable from either data set alone.

Integration of all of these sources of information can raise significant challenges. Modern digital image processing, geographic-information-system (GIS) technology, and neural networks are now used extensively to aid integration efforts. Interpreters typically work on electronic as well as hard-copy maps, using GIS and raster-based imaging software to overlay numerous layers of geologic data together with gravity grids and filtered residual maps. Using these techniques, gravity data are readily integrated into the common earth model and imaged in 3D visionariums for optimal interpretation.

Modern imaging technology has enabled the simultaneous spatial association of multiple kinds of data and information. Interpretation skills now are pushed to a new level in which information from different disciplines is incorporated into a unified geologic understanding of the subsurface. Modern gravity and magnetic interpreters benefit from their knowledge of seismic, well-log, thermal history, and structural information because these data are now integrated with gravity modeling and interpretation on a regular basis.

## CASE HISTORIES

The utility of gravity methods in solving various exploration problems is illustrated by the case histories shown below.

### Albuquerque basin gravity survey, north-central New Mexico

Gravity models were a critical element in a groundwater study of the Albuquerque and neighboring basins in north-central New Mexico (Grauch et al., 2002). The basins formed in response to the development of the Rio Grande rift during the Neogene. During rifting, sediments and minor basalt flows accumulated on top of a basin floor composed of variably eroded older sedimentary rocks overlying the Precambrian basement. The rift-related sediments are now the primary aquifers supplying water for most nonagricultural uses in the Albuquerque metropolitan area. Thus, gravity modeling focused on estimating the thickness of the Neogene sediments rather than the thickness of the entire sedimentary package within the basins.

Gravity modeling was accomplished using a 3D iterative technique developed by Jachens and Moring (1990; described in Blakely and Jachens, 1991). The method assigns different density-depth functions to individual geologic units, thus providing improvements over earlier modeling efforts (Birch, 1982). An iterative process of regional-residual separation and forward calculation using Parker's method (1972) is initiated by gridding only those gravity stations located on outcrops of prerift rocks as the first estimate of the regional field. Adjust-

ments to the rift-fill thickness are then determined via Bott's method (1960) until the regional fields plus the residual fields match the observed data and the model fits all independent constraints, such as drill-hole information. The resulting gravity model was combined with faults synthesized from geophysical interpretations and geologic mapping to develop a 3D surface representing the base of the rift fill (Figure 2). This surface ultimately served as the lower limit of a regional groundwater flow model for the entire basin area (McAda and Barroll, 2002).

### Resolving the K-2 salt structure, Gulf of Mexico

Full-tensor gravity gradiometry (FTG) systems possess the resolution and sensitivity required in detailed mapping for mineral, oil, and gas exploration, even for relatively deep objectives. Used in combination with 3D seismic prestack-depth-migration imaging, FTG gravity data provide a potent mapping capability in presalt areas of the deepwater Gulf of Mexico. O'Brien et al. (2005) illustrate this with a subsalt case study from the K-2 field in the Gulf of Mexico, where an integrated approach using seismic wave-equation depth imaging and FTG inversion resolves the base of salt much better than Kirchhoff depth imaging alone.

While a conventional gravity survey records a single component of the three-component gravitational force (usually the vertical component) FTG measures the derivatives of all three components in all three directions. Thus, the method measures the variation of the vertical component of the gravitational force in the vertical direction and in two horizontal directions. Similarly, it measures the variation of the horizontal components of gravity in all three directions. Figure 3

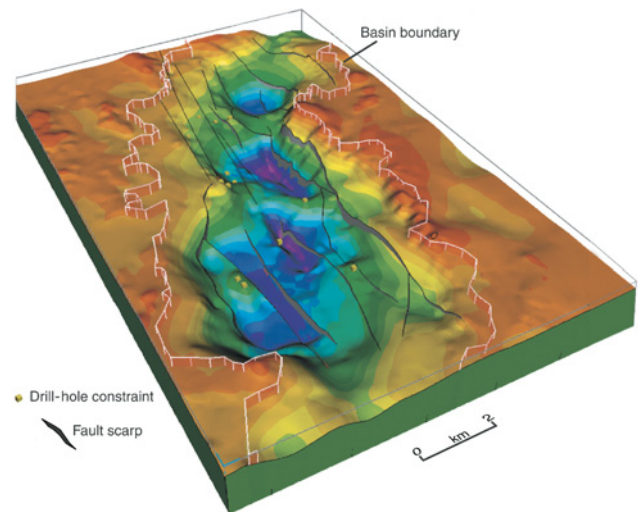


Figure 2. Perspective of a 3D model representing the base of aquifer sediments in the Albuquerque and neighboring basins. Gravity modeling, which focuses on separating the effects of the aquifer thickness from the underlying sedimentary package plus Precambrian basement, uses the iterative technique of Jachens and Moring (1990) constrained by drill-hole information. The model is combined with faults synthesized from geophysical interpretations and geologic mapping to give a 3D surface that ultimately serves as the lower limit of a regional groundwater flow model for the entire basin area. From Grauch et al. (2002).

compares the  $G_{zz}$  (first vertical derivative of gravity) computed from a regular gravity survey (Figure 3a); as measured from the FTG survey (Figure 3b); and as computed from all the FTG vectors (Figure 3c). Note that Figure 3c has higher frequencies, and the subsequent higher-resolution representation of the gravity field can help provide more detail in the base-of-salt structure.

Full integration of 3D seismic data and FTG gravity data is accomplished by first constructing an earth-model cube of structure, velocity, and density. This starting earth model incorporates well control where present and a 3D seismic-velocity cube constructed from an initial 3D seismic interpretation. A 3D FTG gravity model is then computed for the initial starting model. FTG gravity misfits (observed minus computed) larger than the FTG noise level are used to adapt the gravity model until an acceptable fit is obtained. Figure 4 shows a cross section through the K2 discovery with the initial 3D Kirchhoff seismic image (Figure 4a), the image with the base of salt from the FTG model in yellow (Figure 3b), and a wave-equation prestack-depth-migration seismic image derived in an independent study (Figure 4c). The close agreement between the FTG-Kirchhoff solution shown in yellow with that of the wave-equation migration provides a high degree of confidence in the position of the base of salt, allowing the updip limits and, thus, the size of the field to be identified. Without this information, the field-development options would have been (1) to drill an updip well to test whether the reservoir extends into the seismic no data zone (a deepwater well drilled to this depth is expensive and, based on the results of this study, would have been a dry hole) or (2) not to drill updip and possibly leave some stranded pay sands untapped.

### Detecting kimberlite pipes at Ekati with airborne gravity gradiometry

A BHP Billiton high-resolution airborne gravity gradiometry (AGG) survey over the Ekati diamond mine in the Northwest Territories of Canada detected clear gravity anomalies over known and suspected kimberlites (Liu et al., 2001). The airborne survey, the first gravity gradiometry survey conducted for kimberlite exploration, was flown at 80 m flight height above ground on 100-m flight-line spacing. AGG aero-

magnetic, and laser profiler data were collected with a single-engine, fixed-wing system.

The high-resolution laser terrain profiler is important for making terrain corrections since the most significant density contrast and the contrast closest to the airplane is the air-ground interface. Terrain is modeled with a 3D gravity-modeling algorithm using an appropriate density for surface geology. In outcropping granitic areas, a  $2.67\text{-g/cm}^3$  density is appropriate. In areas of local glacial till, a lower density ( $1.6\text{--}2.0\text{ g/cm}^3$ ) is applied. Figure 5 is an image of the vertical gravity gradient from the Ekati survey scaled in Eötvös units. Three known kimberlites are identified as dark spots, corresponding to the lower density of the weathered kimberlite. Near-surface geology is represented by high-density linear dikes in the magnified area below.

In addition to the AGG, gravity gradient measurements can be used to compute gravity. Figure 6 represents the same area as Figure 5 but shows the terrain-corrected vertical component of gravity. The noise level is estimated at 0.2 mGal with a spatial wavelength of 500 m. For this map to conform to either free-air or Bouguer standards, it must be calibrated to tie base-station data points. However, the vertical gravity gradient data are preferred for picking potential targets, especially in kimberlite exploration.

The AGG survey was successful at imaging 55% of the 136 known kimberlites in the survey area. Additional lead areas not previously mapped as kimberlites prior to the survey were subsequently drilled and were found to be kimberlites. Data resolution was determined to be 7 EU with a 300-m wavelength. Tightening the flight line spacing to 50 m in a local test area slightly improved measurement accuracy and improved the horizontal wavelength to less than 300 m. Integration of the high-sensitivity terrain and airborne magnetic data significantly improved the sensitivity of the AGG survey data.

### THE FUTURE

Operating systems will continue to migrate to the widely used Windows™ and Linux™ platforms. Efficient data management will receive more emphasis, and data-retrieval applications will become easier to use. Geophysicists will continue to improve their access to data from remote field offices. Interpretation using detailed and more realistic 3D models with new and improved modeling systems will become more commonplace. Tighter integration with seismic models in potential-field data interpretation will help to improve the seismic-velocity model in a more timely fashion. Joint interpretation with other nonseismic methods such as the emerging marine electromagnetic methods is rapidly finding acceptance in oil companies. New functionalities will take advantage of the additional information and resolution provided by gravity and magnetic gradient data.

Much of what has happened over the last 25 years is a refinement of the major breakthroughs of the preceding 50 years; an example is the steady improvement in

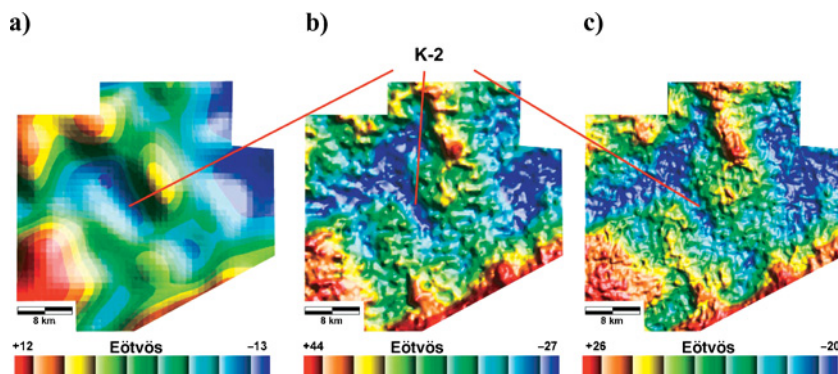


Figure 3.  $G_{zz}$ , the partial derivative with respect to the  $z$ -axis of the vertical force of gravity. (a)  $G_{zz}$  derived from conventional Bouguer gravity. (b)  $G_{zz}$  as measured with an FTG survey. (c) Best estimate of  $G_{zz}$  obtained by using all tensor components.

both marine and airborne gravity operations. Reservoir monitoring and characterization are becoming major activities in the oil and gas industry. By combining the less-expensive relative gravimeters with the calibration of absolute gravimeters,

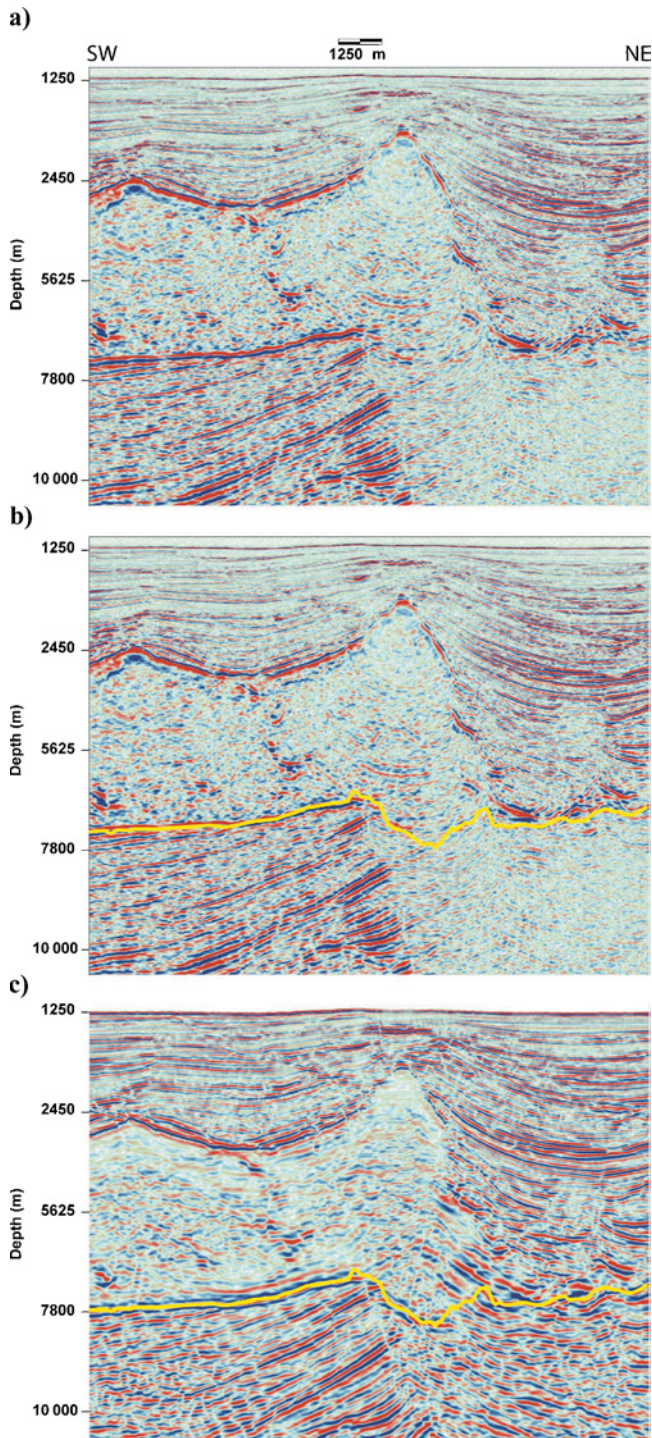


Figure 4. Prestack depth-migration profile along line *B* through the K-2 field. (a) Kirchhoff migration. (b) Kirchhoff migration with base-of-salt horizon shown in yellow, as determined by FTG inversion. (c) Wave-equation prestack depth migration, which also shows the presence of a salt keel. Yellow horizon shows the FTG inversion result.

corrected for tidal effects. Reservoir monitoring may introduce an entirely new and robust activity for gravity specialists.

The present pace of technical innovation will likely continue into the future, with maximum sensor resolution moving well into the submicrogal range. The time it takes to make a high-resolution measurement will continue to become shorter — 1 min or less to make a  $1\text{-}\mu\text{Gal}$  resolution measurement

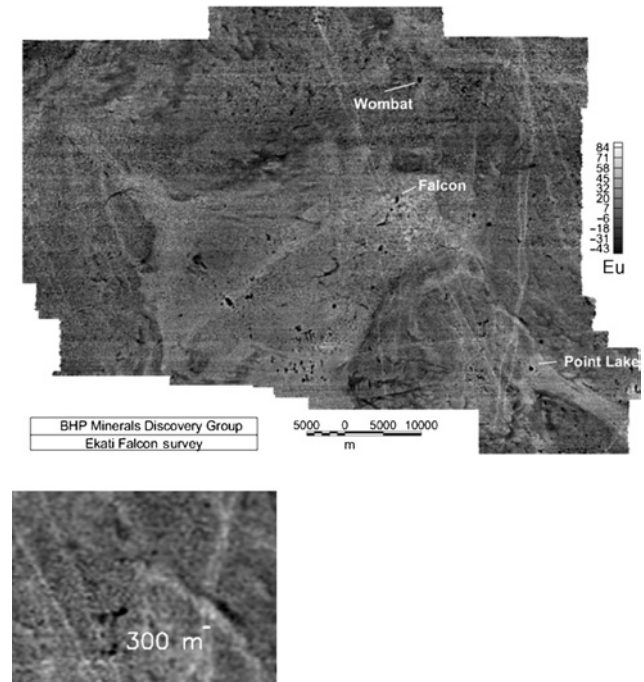


Figure 5. Vertical gravity gradient  $G_{zz}$  from the Ekati survey. The upper figure is a shaded relief image of  $G_{zz}$  with vertical scale as dark (negative, local low-density features) to white (positive, local high-density features). The image below is an enlarged section of the southeastern part of the image. Two higher-density (white) dikes separated at just over 300 m are resolved on the lower image. The white bar has a horizontal dimension of 300 m.

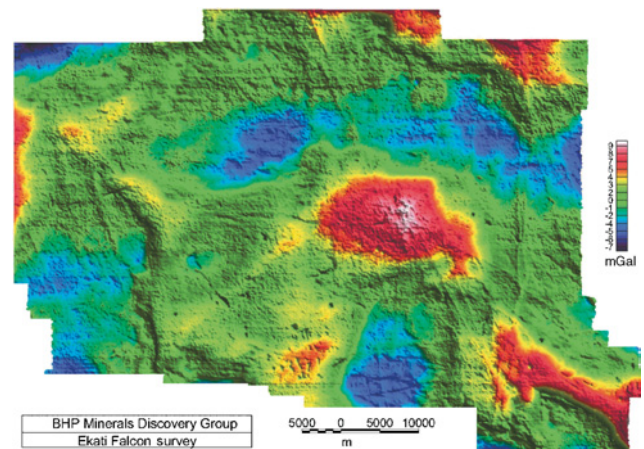


Figure 6. Vertical gravity  $G_z$  as a color-shaded image from the Ekati survey.  $G_z$  is the equivalent to terrain-corrected Bouguer gravity in mGal.

may soon be a reality. Gravity sensors should become much smaller in the near future, and gravimeters will continue to become more automated and easier to operate. As free-fall technology continues to get smaller, faster, and less expensive, free-fall instruments will become more competitive with spring gravimeters. These changes are being driven by the need to place gravity sensors in petroleum wells for exploration and production monitoring purposes. The development of gravity-measurement-while-drilling and gravity-array technology is on the horizon. These advancements will lead to the development of new geophysical applications and more advanced integration of gravity and seismic data.

Many of the interpretation models in the major oil companies will start at the Moho (or, in some cases, even below the Moho) and extend right to the surface. These will include situations where the stakes are high, and there are many constraints in addition to gravity data.

As AGG becomes more robust, we can anticipate significant reductions in the cost of surveying and more flexibility in the airborne platforms used for acquisition. Ultimately, airborne gradiometry may supplant land-based acquisition, as it will be so much faster, more uniformly sampled, still very accurate, and reasonably priced.

GPS elevation measurements, which are referenced to the ellipsoid rather than the geoid, will make it increasingly likely that the ellipsoid will supplant the geoid as the standard reference surface. By using the ellipsoid and GPS locations, gravity surveys can be conducted in areas where traditional geoid elevations are unavailable or unreliable.

Finally, expect the unexpected. With the tremendous pace of advancements in atomic and solid-state physics, as well as microprocessing and materials engineering, advancements in new technologies could have a significant impact of the future of gravity instrumentation. There is already a long list of diverse types of technology proposed for gravimeters, such as fluid float, atomic fountain, atomic spectroscopy, vibrating quartz beam, photoelastic torqued elements, spinning torqued elements, superradiant spectroscopy, vibrating beam, sapphire resonator, piezoelectric, and electrochemical, with undoubtedly more to come.

**ACKNOWLEDGMENTS**

The authors sincerely thank Mark Dransfield for supplying images and information of the case history on the gravity gradiometry survey over the Ekati diamond mine and Mark Davies for supplying information and images for the case history of the K-2 salt structure in the Gulf of Mexico. The manuscript benefited greatly from thoughtful and in-depth reviews by William Hinze, Dhananjay Ravat, Rick Saltus, Manik Talwani, and Mike Webring.

The authors made a serious effort to include in this paper all pertinent developments and references related to the historical development of the gravity method. In a paper of this magnitude, it is inevitable that we may have missed some. This was unintentional, and we apologize for any unintended omissions.

**APPENDIX A**

**TIMELINE OF GRAVITY EXPLORATION**

Date	Event	Date	Event
1604	Galileo — Inclined plane experiments	1932	Hartley gravity meter — Early published description
1656	Huygens — First pendulum clock and its use to measure absolute gravity	1934	LaCoste — Zero-length spring
1687	Newton — Inverse square law	1939	Hammer — Terrain corrections for exploration
1733	Clairaut — Theoretical earth gravity	1941	Gulf Oil — Ocean-bottom gravimeter
1749	Bouguer — La figure de la terre	1942	Nettleton (and Bardeen) — Treatment of solid angles
1799	Laplace — Mecanique Celeste	1944	Sellers — Diving bell gravity measurements
1812	Poisson — Attracting matter	1947	Frowe — Diving bell underwater exploration
1817	Kater — Reversible pendulum	1947	Skeels — Clear statement of ambiguity
1819	Young — Gravity reduction	1950	LaCoste and Romberg — seismically compensated underwater meter
1828	Green — Equivalent layer	1949	Henderson and Zietz — Computation of second vertical derivatives
1829	MacCullagh — Moments of inertia	1949	Gilbert — Vibrating-string gravimeters
1833	Herschel — Proposed using a spring balance to measure gravity	1950	Smith — The case for borehole gravity measurements
1878	Von Jolly — Gravitational constant	1951	Elkins — Second vertical derivative calculations
1888	Eötvös — Torsion balance	1955	Askania — Surface-ship gravity meter without cross-coupling
1906	Absolute gravity measurement (Potsdam)	1958	Dean — Use of Fourier transform in potential field data analysis
1909	Hayford — Terrain corrections and Isostatic reductions	1959	Talwani, Worzel and Landisman-Rapid 2D gravity and magnetic modeling
1915	Schweydar — First exploration use of torsion balance	1960	Talwani and Ewing — Three-dimensional digital gravity calculation
1924	Discovery of the Nash Dome, Texas (using torsion balance)	1960	Bott — Iterative inversion of gravity and magnetic data
1930	Heyl — Refined gravitational constant	1960s	U. S. Navy — First modern gravity gradiometer
1930	Gulf Oil Company — Pendulum surveys for oil	1962	Bowin — First marine gravity system with an automated digital acquisition system

Date	Event	Date	Event
1963	Hammer — Deep gravity interpretation by stripping	1975	Parker — Theory of ideal bodies
1964	Goodell and Fay — Shell vibrating-string gravimeter	1977	Bhattacharyya and Chan — Computations with inhomogeneous density
1965	LaFehr and Nettleton — L&R surface-ship test with cross-coupling	1978	LaCoste and Romberg — Slimhole borehole gravimeter
1965	LaCoste and Romberg — borehole gravimeter	1979	Cordell — Horizontal gradient method
1965	Bhattacharyya — Fourier analysis	1980	Carson Helicopters — Start of airborne gravity
1965	Cooley and Tukey — Development of fast Fourier transform (FFT)	1980s	U. S. Air Force — Airborne gravity gradiometer development
1966	Esso — First instrument to measure gravity in a borehole	1980s	Postprocessing of differential GPS navigation
1966	Bell Instruments — Electromagnetic restoring principle	1982	Seasat — Satellite altimetry
1967	Fuller — Analysis of space-domain filters	1984	Goupillaud et al. — Wavelet transforms
1967	Bhattacharyya — Review of general properties of potential fields	1987	First time gravity data taken with GPS
1970	Spector and Grant — Power spectrum depth estimation	1990s	Real-time GPS navigation increases quality of corrections for platform motion
1971	Morelli, et al. — Gravity standardization net	1992	LaFehr, Valliant, and MacQueen — High-resolution marine gravity by digital control
1972	Wiggins — General inversion	1993	Phillips — Matched Wiener filtering as depth-related bandpass
1972	Parker — Fourier modeling of complex topography	1994	First commercial FTG measurements at sea
1972	Syberg — Potential-field continuation and matched filters	1994	First absolute gravity measurements for reservoir monitoring on North Slope
1972	First gravity measurements on the moon	1997	Falcon — Airborne horizontal gravity gradient system
1973	Apollo 17 — Gravity measurements on the moon	1997	Moreau et al. — Wavelet analysis of potential fields
1974	Briggs — Minimum curvature gridding	1998	Li and Oldenburg — 3D inversion of gravity data

## REFERENCES

- Agarwal, R. G., and E. R. Kanasewich, 1971, Automatic trend analysis and interpretation of potential field data: *Geophysics*, **36**, 339–348.
- Agocs, W. B., 1951, Least-squares residual anomaly determination: *Geophysics*, **16**, 686–696.
- Airy, G. B., 1855, On the computation of the effect of the attraction of mountain-masses, as disturbing the apparent astronomical latitude of stations in geodetic surveys: *Philosophical Transactions of the Royal Society of London*, **145**, 101–104.
- Alexander, M., and K. O. Heintz, 1998, Sulfur exploration with core-hole and surface gravity in R. I. Gibson and P. S. Milligan, eds., *Geologic applications gravity and magnetics: Case histories: SEG Geophysical Reference Series 8 and American Association of Petroleum Geologists, AAPG Studies in Geology*, **43**, 113–119.
- Ander, M. E., T. Summers, and M. Gruchalla, 1999, The LaCoste & Romberg gravity meter: System analysis and instrumental errors: *Geophysics*, **64**, 1708–1819.
- Barbosa, V. C. F., J. B. C. Silva, and W. E. Medeiros, 1997, Gravity inversion of basement relief using approximate equality constraints on depths: *Geophysics*, **62**, 1745–1757.
- Barnett, C. T., 1976, Theoretical modeling of the magnetic and gravitational fields of an arbitrarily shaped three-dimensional body: *Geophysics*, **41**, 1353–1364.
- Barton, D. C., 1928, The Eötvös torsion balance method of mapping geologic structure: American Institute of Mining Metallurgy and Engineering Technical Publication 50.
- Bhattacharyya, B. K., 1965, Two-dimensional harmonic analysis as a tool for magnetic interpretation: *Geophysics*, **30**, 829–857.
- , 1967, Some general properties of potential fields in space and frequency domain: A review: *Geoexploration*, **5**, 127–143.
- Bhattacharyya, B. K., and K. C. Chan, 1977, Computation of gravity and magnetic anomalies due to inhomogeneous distribution of magnetization and density in a localized region: *Geophysics*, **42**, 602–609.
- Birch, F. S., 1982, Gravity models of the Albuquerque basin, Rio Grande rift, New Mexico: *Geophysics*, **47**, 1185–1197.
- Blakely, R. J., 1995, *Potential theory in gravity and Magnetic Applications*: Cambridge University Press.
- Blakely, R. J., and R. C. Jachens, 1991, Regional study of mineral resources in Nevada: Insights from three-dimensional analysis of gravity and magnetic anomalies: *Bulletin of the Geological Society of America*, **103**, 795–803.
- Blakely, R. J., and R. W. Simpson, 1986, Approximating edges of source bodies from magnetic or gravity anomalies: *Geophysics*, **51**, 1494–1498.
- Bott, M. H. P., 1959, The use of electronic digital computers for the evaluation of gravimetric terrain corrections: *Geophysical Prospecting*, **7**, 45–54.
- , 1960, The use of rapid digital computing methods for direct gravity interpretation of sedimentary basins: *Geophysical Journal of the Royal Astronomical Society*, **3**, 63–67.
- Bowin, C., T. C. Aldrich, and R. A. Folinsee 1972, VSA gravity meter system: Tests and recent developments: *Journal of Geophysical Research* **77**, 2018–2033.
- Bradley, J. W., 1974, The commercial application and interpretation of the borehole gravimeter: Contemporary Geophysical Interpretation Symposium, Geophysical Society of Houston, Proceedings.
- Breiner, S., J. D. Corbett, J. J. Daniels, D. A. Hansen, R. F. Horsnail, and H. F. Morrison, 1981, American mining geophysics delegation to the People's Republic of China: *Geophysics*, **46**, 347–356.
- Briggs, I. C., 1974, Machine contouring using minimum curvature: *Geophysics*, **39**, 39–48.
- Brissaud, P., P. Deletie, J. Lakshmanan, Y. Lemoine, and J. Montlucou, 1989, Site of Tanis (Egypt): Geophysical investigations and their archaeological follow-up: 59th Annual International Meeting, SEG, Expanded Abstracts, 292–293.
- Brown, J. M., F. J. Klopping, D. van Westrum, T. M. Niebauer, R. Billson, J. Brady, J. Ferguson, T. Chen, and J. Siebert, 2002, Preliminary absolute gravity survey results from water injection monitoring program at Prudhoe Bay: 72nd Annual International Meeting, SEG, Expanded Abstracts, 791–793.
- Brown, J. M., T. M. Niebauer, B. Richter, F. J. Klopping, J. G. Valentine, and W. K. Buxton 1999, Miniaturized gravimeter may greatly improve measurements: EOS, Transactions of the American Geophysical Union, <[http://www.agu.org/eos\\_elec/99144e.html](http://www.agu.org/eos_elec/99144e.html)>.
- Byerly, P. E., 1965, Convolution filtering of gravity and magnetic maps: *Geophysics*, **30**, 281–283.
- Cady, J. W., 1980, Calculation of gravity and magnetic anomalies of finite-length right polygonal prisms: *Geophysics*, **45**, 1507–1512.
- Carmichael, R. S., 1984, *CRC handbook of physical properties of Rocks*: CRC Press.
- Cazenave, A., and J.-Y. Royer, 2001, Applications to marine Geophysics, in L. L. Fu and A. Cazenave, eds., *Satellite altimetry and earth sciences*: Academic Press, 407–435.

- Cazenave, A., P. Schaeffer, M. Berge, and C. Brossier, 1996, High-resolution mean sea surface computed with altimeter data of ERS-1 (Geodetic Mission) and TOPEX-Poseidon: *Geophysical Journal International*, **125**, 696–704.
- Ceron, J., T. R. Horscroft, and J. E. Bain, 1997, Airborne gravity and magnetic interpretation of the Putumayo and Upper Magdalena Valley, Colombia: 67th Annual International Meeting, SEG, Expanded Abstracts, 707–709.
- Chai, Y., and W. J. Hinze, 1988, Gravity inversion of an interface above which the density contrast varies exponentially with depth: *Geophysics*, **53**, 837–845.
- Chapin, D. A., 1996, The theory of the Bouguer gravity anomaly: A tutorial: *The Leading Edge*, **15**, 361–363 (discussion in **15**, 808 and 1216).
- , 1997, Wavelet transforms: A new paradigm for interpreting gravity and magnetics data?: 67th Annual International Meeting, SEG, Expanded Abstracts, 486–489.
- , 1998a, The isostatic gravity residual of onshore South America: Examples of the utility of isostatic gravity residuals as a regional exploration tool, in R. I. Gibson and P. S. Millegan, eds., *Geologic applications of gravity and magnetics: Case histories: SEG Geophysical Reference Series 8, and AAPG Studies in Geology 43*, 34–36.
- , 1998b, Gravity instruments: Past, present, future: *The Leading Edge*, **17**, 100–112.
- , 2000, Gravity measurements on the moon: *The Leading Edge*, **19**, 88–90.
- Chapin, D. A., and M. E. Ander, 1999a, Applying gravity to petroleum exploration in E. A. Beaumont and N. H. Foster, eds., *Exploring for oil and gas traps: American Association of Petroleum Geologists*.
- , 1999b, Borehole gravity: New life for borehole gravity?: *AAPG Explorer*, **20**, 24–29.
- Cheng, D., Y. Li, and K. Lerner, 2003, Inversion of gravity data for base salt: 73rd Annual International Meeting, SEG, Expanded Abstracts, 588–591.
- Clark, R. D., 1984, Lucien LaCoste: *The Leading Edge*, **3**, 24–29.
- Clarke, G. K. C., 1969, Optimum second derivative and downward continuation filters: *Geophysics*, **34**, 424–437.
- Cooper, G. R. J., and D. R. Cowan, 2003, The meter reader—Sunshading geophysical data using fractional order horizontal gradients: *The Leading Edge*, **22**, 204.
- Cordell, L., 1979, Gravimetric expression of graben faulting in Santa Fe County and the Espanola basin, New Mexico, in R. V. Ingersoll, ed., *Guidebook to Santa Fe County: New Mexico Geological Society*, 59–64.
- , 1985, Applications and problems of analytical continuation of New Mexico aeromagnetic data between arbitrary surfaces of very high relief: International Meeting on Potential Fields in Rugged Topography, Institute de Geophysique de Universite de Lausanne, Proceedings, 96–101.
- , 1992, A scattered equivalent-source method for interpolation and gridding of potential-field data in three dimensions: *Geophysics*, **57**, 629–636.
- Cordell, L., and V. J. S. Grauch, 1982, Mapping basement magnetization zones from aeromagnetic data in the San Juan Basin, New Mexico: 52nd Annual International Meeting, SEG, Expanded Abstracts, 246–247.
- , 1985, Mapping basement magnetization zones from aeromagnetic data in the San Juan Basin, New Mexico, in W. J. Hinze, ed., *Utility of regional gravity and magnetic maps: SEG*, 181–197.
- Cordell, L., and A. E. McCafferty, 1989, A terracing operator for physical property mapping with potential field data: *Geophysics*, **54**, 621–634.
- Cordell, L., Y. A. Zorin, and G. R. Keller, 1991, The decompensative gravity anomaly and deep structure of the region of the Rio Grande rift: *Journal of Geophysical Research*, **96**, 6557–6568.
- Cowan, D.R., and S. Cowan, 1993, Separation filtering applied to aeromagnetic data: *Exploration Geophysics*, **24**, 429–436.
- Craig, M., 1996, Analytic signals for multivariate data: *Mathematical Geology*, **28**, 315–329.
- Danes, Z. F., 1960, On a successive approximation method for interpreting gravity anomalies: *Geophysics*, **25**, 1215–1228.
- Dean, W. C., 1958, Frequency analysis for gravity and magnetic interpretation: *Geophysics*, **23**, 97–127.
- Deletie, P., Y. Lemoine, J. Montlucon, and J. Lakshmanan, 1988, Discovery of two unknown pyramids at Saqqarah, Egypt by a multithod geophysical survey: 58th Annual International Meeting, SEG, Expanded Abstracts, 335–337.
- DiFrancesco, D., and M. Talwani, 2002, Time-lapse gravity gradiometry for reservoir monitoring: 72nd Annual International Meeting, SEG, Expanded Abstracts, 787–790.
- Dobrin, M. B. 1960, Introduction to geophysical prospecting, 2nd ed: McGraw-Hill Book Company.
- , 1976, Introduction to geophysical prospecting, 3rd ed: McGraw-Hill Book Company.
- Eaton, D., and K. Vasudevan, 2004, Skeletonization of aeromagnetic data: *Geophysics*, **69**, 478–488.
- Ecker, E., and E. Mittermayer, 1969, Gravity corrections for the influence of the atmosphere: *Bulletin of Theoretical and Applied Geophysics*, **11**, 70–80.
- Eckhardt, D. H., 1986, Status of the gravity gradiometer survey system, Bureau Gravimetrique International, **59**, 81–87.
- Eckhardt, E. A., 1940, A brief history of the gravity method of prospecting for oil: *Geophysics*, **5**, 231–242.
- Elieff, S., 2003, Project report for an airborne gravity evaluation survey, Timmins, Ontario: Report produced for Timmins Economic Development Corp. on behalf of the Discover Abitibi Initiative, <<http://www.discoverabiti.com/technical-projects.htm>>.
- Elieff, S., and S. Sander, 2004, The AIRGrav airborne gravity survey in Timmins, Ontario: Airborne Gravity Workshop, Australian Society of Geophysicists, Preprints, <[http://www.ga.gov.au/rural/projects/index\\_2004\\_18.jsp](http://www.ga.gov.au/rural/projects/index_2004_18.jsp)>.
- Faller, J. E., 2002, Thirty years of progress in absolute gravimetry: A scientific capability implemented by technological advances: *Metrologia*, **39**, no. 5, 425–428.
- Frowe, E. W., 1947, A diving bell for underwater gravimeter operation: *Geophysics*, **12**, 1–12.
- Fuller, B. D., 1967, Two-dimensional frequency analysis and design of grid operators: *Mining Geophysics*, **2**, 658.
- Gay, M. W., 1940, Relative gravity measurements using precision pendulum equipment: *Geophysics*, **5**, 176–193.
- Gibson, R. I., 1998, Utility in exploration of continent-scale data sets, in R. I. Gibson, and P. S. Millegan, eds. *Geologic applications of gravity and magnetics: Case histories: SEG Geophysical Reference Series 8 and AAPG Studies in Geology 43*, 32–33.
- Gilbert, R. L., 1949, A dynamic gravimeter of novel design: Proceedings of the Physical Society of London, Series. B, **62**, 445–454.
- Götze, H. J., Ö. Rosenbach, and W. Schöler, 1976, Zur Reproduzierbarkeit von Vertikalgradientenmessungen: *Österreichische Zeitschrift für Vermessungswesen und Photogrammetrie*, **63**, 146–157.
- Goupillaud, P. L., A. Grossmann, and J. Morlet, 1984, Cycle-octave and related transforms in seismic signal analysis: *Geoexploration*, **23**, 85–102.
- Goussev, S. A., R. A. Charters, J. W. Peirce, and W. E. Glenn, 2003, The meter reader — Jackpine magnetic anomaly: Identification of a buried meteorite impact structure: *The Leading Edge*, **22**, 740–741.
- Graf, A., 1958, Das seegravimeter: *Zeitschrift Instrumenten Kunde*, **60**, 151–162.
- Granser, H., B. Meurers, and P. Steinhäuser, 1989, Apparent density mapping and 3D gravity inversion in the eastern Alps: *Geophysical Prospecting*, **37**, 279–292.
- Grant, F. S., 1973, The magnetic susceptibility mapping method for interpreting aeromagnetic surveys: *Geophysics*, **38**, 1201(abstract).
- Grant, F. S., and A. F. Elsharty, 1962, Bouguer gravity corrections using a variable density: *Geophysics*, **27**, 616–626.
- Grauch, V. J. S., and L. Cordell, 1987, Limitations on determining density or magnetic boundaries from the horizontal gradient of gravity or pseudogravity data: *Geophysics*, **52**, 118–121.
- Grauch, V. J. S., and C. S. Johnston, 2002, Gradient window method: A simple way to separate regional from local horizontal gradients in gridded potential-field data: 72nd Annual International Meeting, SEG, Expanded Abstracts, 762–765.
- Grauch, V. J. S., B. D. Rodriguez, and M. Deszcz-Pan, 2002, How geophysical methods have been used to understand the subsurface, in J. R. Bartolino, and J. C. Cole, eds., *Ground-water resources of the middle Rio Grande basin, New Mexico U. S. Geological Survey Circular 1222*, 36–37.
- Green, W. R., 1975, Inversion of gravity profiles by use of a Backus-Gilbert approach: *Geophysics*, **40**, 763–772 (discussion in **41**, 777; reply in **41**, 777–778).
- Greene, E. F., and C. M. Bresnahan, 1998, Gravity's role in a modern exploration program, in R. I. Gibson and P. S. Millegan, eds., *Geologic applications of gravity and magnetics: Case histories: SEG Geophysical Reference Series 8 and AAPG Studies in Geology 43*, 9–12.
- Griffins, W. R., 1949, Residual gravity in theory and practice: *Geophysics*, **14**, 39–56.
- Guillen, A., and V. Menichetti, 1984, Gravity and magnetic inversion with minimization of a specific functional: *Geophysics*, **49**, 1354–1360.
- Guspi, F., 1992, Three-dimensional Fourier gravity inversion with arbitrary density contrast: *Geophysics*, **57**, 131–135.

- Guspi, F., and B. Introcaso, 2000, A sparse spectrum technique for gridding and separating potential field anomalies: *Geophysics*, **65**, 1154–1161.
- Haalck, H., 1939, Der statische (barometrische) Schweremesser für Messungen auf festem Lande und auf See (A static [barometric] gravity meter for measurements on land and sea): *Beitrage Zeitschrift für Angewandte Geophysik*, **7**, 285–316, 392–448.
- Hammer, S., 1939, Terrain corrections for gravimeter stations: *Geophysics*, **4**, 184–194.
- , 1950, Density determination by underground gravity measurements: *Geophysics*, **15**, 637–652.
- , 1963, Deep gravity interpretation by stripping: *Geophysics*, **28**, 369–378.
- , 1983, Airborne gravity is here!: *Geophysics*, **48**, 213–223; discussion and replies in **49**, 310–311, 470–477; **50**, 170–171; **51**, 1502–1503; **52**, 376; letter in **49**, 1814–1814.
- Hansen, R. O., 1993, Interpretative gridding by anisotropic kriging: *Geophysics*, **58**, 1491–1497.
- , 2001, Gravity and magnetic methods at the turn of the millennium: *Geophysics*, **66**, 36–37.
- Hansen, R. O., and Y. Miyazaki, 1984, Continuation of potential fields between arbitrary surfaces: *Geophysics*, **49**, 787–795.
- Harrison, J. C., 1959, Tests of the LaCoste-Romberg surface ship gravity meter: *Journal of Geophysical Research*, **64**, 1875–1881.
- , 1995, Memorial — Lucien LaCoste: *The Leading Edge*, **14**, 1002–1003.
- Haxby, W. F., G. D. Karner, J. L. LaBrecque, and J. K. Weisell, 1983, Digital images of combined oceanic and continental data sets and their use in tectonic studies: EOS, *Transactions of the American Geophysical Union*, **64**, 995–1004.
- Hayford, J. F., and W. Bowie, 1912, The effect of topography and isostatic compensation upon the intensity of gravity: U.S. Coast and Geodetic Survey Publication 10.
- Hecker, O., 1903, Bestimmung der schwerkraft auf dem Atlantischen Ozean, sowie in Rio de Janeiro, Lissabon, und Madrid (Determination of gravity in the Atlantic Ocean and also at Riode Janeiro, Lisbon and Madrid): Veröffentlichung königlich Preussische Geodätische Institut Research Volume II.
- Heiskanen, W. A., and F. A. V. Meinesz, 1958, *The earth and its gravity field*: McGraw-Hill Book Company.
- Helmert, F. R., 1884, *Die mathematischen und physikalischen Theorien der höheren Geodäsie* (The mathematical and Physical theory of advanced geodesy): Teubner (reprinted by Minerva, 1962).
- , 1890, *Die Schwerkraft im Hochgebirge, insbesondere in den Tyroler Alpen* (Gravity in high mountains, especially the Tyroler Alps): Veröffentlichung Königlich Preußische Geodätische Institut Research Volume I.
- Henderson, R., 1960, A comprehensive system of automatic computation in magnetic and gravity interpretation: *Geophysics*, **25**, 569–585.
- Henderson, R. G., and I. Zietz, 1949, The computation of second vertical derivatives of geomagnetic fields: *Geophysics*, **14**, 508–516.
- Hildenbrand, T. G., A. Briesacher, G. Flanagan, W. J. Hinze, A. M. Hittelman, G. R. Keller, R. P. Kucks, D. Plouff, W. R. Roest, J. Seeley, et al., 2002, Rationale and operational plan to upgrade the U.S. gravity database: U. S. Geological Survey Open-file Report 02–463.
- Hinze, W. J., ed., 1985, *The utility of regional gravity and magnetic anomaly maps*: SEG.
- Hinze, W. J., 1991, The role of gravity and magnetic methods in engineering and environmental studies, in S. H. Ward, ed., *Geotechnical and environmental Geophysics I: Review and tutorial*: SEG, 75–126.
- Hinze, W. J., C. Aiken, J. Brozena, B. Coakley, D. Oater, G. Flanagan, R. Forsberg, T. Hildebrand, G. R. Keller, J. Kellogg, et al., 2005, New standards for reducing gravity data: The North American gravity database: *Geophysics*, **70**, J25–J32.
- Hjelt, S. E., 1974, The gravity anomaly of a dipping prism: *Geoplot*, **12**, 29–39.
- Hornby, P., F. Boschetti, and F. G. Horowitz, 1999, Analysis of potential field data in the wavelet domain: *Geophysical Journal International*, **137**, 175–196.
- Howell, L. G., K. O. Heinze, and A. Perry, 1966, The development and use of a high-precision downhole gravity meter: *Geophysics*, **31**, 764–772.
- Huston, D. C., H. H. Huston, and E. Johnson, 2004, Geostatistical integration of velocity cube and log data to constrain 3D gravity modeling, deepwater Gulf of Mexico: *The Leading Edge*, **23**, 842–846.
- Hwang, C., E.-C. Kao, and B. E. Parsons, 1998, Global derivation of marine gravity anomalies from Seasat, Geosat, ERS-1 and TOPEX/Poseidon altimeter data: *Geophysical Journal International*, **134**, 449–459.
- International Association of Geodesy, 1971, *Geodetic Reference System 1967: Special Publication 3*.
- Jachens, R. C., and B. C. Moring, 1990, Maps of the thickness of Cenozoic deposits and the isostatic residual gravity over basement for Nevada: U. S. Geological Survey Open-File Report 90-404.
- Jachens, R. C., and C. W. Roberts, 1981, Documentation of a FORTRAN program, 'isocomp,' for computing isostatic residual gravity: U. S. Geological Survey Open-File Report 81-574.
- Jacobsen, B. H., 1987, A case for upward continuation as a standard separation filter for potential field maps: *Geophysics*, **52**, 1138–1148.
- Jacques, J. M., M. E. Parsons, A. D. Price, and D. M. Schwartz, 2003, Improving geologic understanding with gravity and magnetic data: Examples from Gabon, Nigeria and the Gulf of Mexico: *First Break*, **21**, no. 11, 57–62.
- Jekeli, C., 1988, The gravity gradiometer survey system (GGSS): EOS, **69**, no. 8, 116–117.
- Jessell, M. W., 2001, Three-dimensional modeling of potential-field data: *Computers & Geosciences*, **27**, 455–465.
- Jessell, M. W., and Fractal Geophysics Pty. Ltd., 2001, An atlas of Structural geophysics II: *Journal of the Virtual Explorer*, <<http://virtualexplorer.com.a4/2001/volume5>>.
- Jessell, M. W., and R. K. Valenta, 1996, Structural geophysics: Integrated structural and geophysical mapping, in D. DePaor, ed., *Structural geology and personal computers*: Elsevier Publishing Company, 303–324.
- Jessell, M. W., R. K. Valenta, G. Jung, J. P. Cull, and A. Gerio, 1993, Structural geophysics: *Exploration Geophysics*, **24**, 599–602.
- Jorgensen, G., and J. Kisabeth, 2000, Joint 3D inversion of gravity, magnetic, and tensor gravity fields for imaging salt formations in the deepwater Gulf of Mexico: 70th Annual International Meeting, SEG, Expanded Abstracts, 424–426.
- Kane, M. F., 1960, Terrain corrections using an electronic digital computer: U. S. Geological Survey Professional Paper 400-B, 132–133.
- , 1962, A comprehensive system of terrain corrections using a digital computer: *Geophysics*, **27**, 455–462.
- Kater, H., 1818, An account of experiments for determining the length of the pendulum vibrating seconds in the latitude of London: *Philosophical Transactions of the Royal Society of London*, **108**, 33–102.
- Keating, P., 1992, Density mapping from gravity data using the Walsh transform: *Geophysics*, **57**, 637–642.
- Kellogg, O. D., 1953, *Foundations of potential theory*: Dover Publishing Inc.
- Krahenbuhl, R., and Y. Li, 2002, Gravity inversion using a binary formulation: 72nd Annual International Meeting, SEG, Expanded Abstracts, 755–758.
- , 2004, Hybrid optimization for a binary inverse problem: 74th Annual International Meeting, SEG, Expanded Abstracts, 782–785.
- LaCoste, L. J. B., 1934, A new type of long-period vertical seismograph: *Physics*, **5**, 178–180.
- , 1959, Surface ship gravity measurements on the Texas A&M College ship, the *Hidalgo*: *Geophysics*, **24**, 309–322.
- , 1967, Measurements of gravity at sea and in the air: *Reviews of Geophysics*, **5**, 477–526.
- , 1988, The zero-length spring gravity meter: *The Leading Edge*, **7**, 20–24.
- LaCoste, L. J. B., N. Clarkson, and G. Hamilton, 1967, LaCoste and Romberg stabilized platform shipboard gravity meter: *Geophysics*, **32**, 99–109.
- LaFehr, T. R., 1980, History of geophysical exploration — Gravity method: *Geophysics*, **45**, 1634–1639.
- , 1983, Rock density from borehole gravity surveys: *Geophysics*, **48**, 341–356.
- , 1991a, Standardization in gravity reduction: *Geophysics*, **56**, 1170–1178.
- , 1991b, An exact solution for the gravity curvature (Bullard B) correction: *Geophysics*, **56**, 1179–1184.
- , 1998, On Talwani's "Errors in the total Bouguer reduction": *Geophysics*, **63**, 1131–1136 (discussion with reply by author in **64**, 988).
- LaFehr, T. R., and K. C. Chan, 1986, Discussion of "The normal vertical gradient of gravity (short note)", by J. H. Karl, (*Geophysics*, **48**, 1011–1013): *Geophysics*, **51**, 1505–1508.
- LaFehr, T. R., and L. L. Nettleton, 1967, Quantitative evaluation of a stabilized platform shipboard gravity-meter: *Geophysics*, **32**, 110–118.
- LaFehr, T. R., V. C. Dean, T. L. Davis, and F. J. Hilterman, 1983, Seismic and gravity modeling of the Mors salt dome, Denmark: 53rd Annual International Meeting, SEG, Expanded Abstracts, 301–303.
- Lakshmanan, J., and J. Montlucon, 1987, Microgravity probes the Great Pyramid: *The Leading Edge*, **6**, 10–17.

- Last, B. J. J., and K. Kubik, 1983, Compact gravity inversion: Geophysics, **48**, 713–721.
- Lee, J. B., 2001, FALCON gravity gradiometry technology: Exploration Geophysics, **32**, 247–250.
- Li, X., 2001, Vertical resolution: Gravity versus vertical gravity gradient: The Leading Edge, **20**, 901–904.
- Li, X. and H. J. Götze, 2001, Ellipsoid, geoid, gravity, geodesy, and geophysics: Geophysics **66**, 1660–1668.
- Li, Y. and D. W. Oldenburg, 1997, Fast inversion of large scale magnetic data using wavelets: SEG, Expanded Abstracts, **16**, 490–493.
- , 1998, 3-D inversion of gravity data: Geophysics, **63**, 109–119.
- , 1999, Rapid construction of equivalent sources using wavelets: 69th Annual International Meeting, SEG, Expanded Abstracts, 374–377.
- , 2003, Fast inversion of large-scale magnetic data using wavelet transforms and logarithmic barrier method: Geophysical Journal International, **152**, 251–265.
- Liu, G., P. Diorio, P. Stone, G. Lockhart, A. Christensen, N. Fitton, and M. Dransfield, 2001, Detecting kimberlite pipes at Ekati with airborne gravity gradiometry: 15th Conference, Australian Society of Exploration Geophysicists, Extended Abstracts.
- Lockwood, A., 2004, Isostatic and decompensative gravity anomalies over Western Australia: Preview, **108**, 22–23.
- Lozhinskaya, A. M., 1959, The string gravimeter for measurement of gravity at sea: Bulletin of the Academy of Sciences USSR Geophysics Series, **3**, 398–409.
- Luyendyk, B. P., 1984, On-bottom gravity profile across the East Pacific crest at 21° north: Geophysics, **49**, 2166–2177.
- Lyman, G. D., C. L. V. Aiken, A. Cogbill, M. Balde, and C. Lide, 1997, Terrain mapping by reflectorless laser ranging systems for inner zone gravity terrain corrections: 67th Annual International Meeting, SEG Expanded Abstracts, 482–485.
- Lyrio, J. C. S., L. Tenorio, and Y. Li, 2004, Efficient automatic denoising of gravity gradiometry data: Geophysics, **69**, 772–782.
- Marlet, G., P. Salliac, F. Moreau, and M. Diament, 2001, Characterization of geological boundaries using 1-D wavelet transform on gravity data: Theory and application to the Himalayas: Geophysics, **66**, 1116–1129.
- McAda, D. P. and P. Barroll, 2002, Simulation of ground-water flow in the Middle Rio Grande basin between Cochiti and San Acacia, New Mexico: U. S. Geological Survey Water-Resources Investigations Report 02-4200.
- McCulloh, T. H., 1965, A confirmation by gravity measurements of an underground density profile based on core densities: Geophysics, **30**, 1108–1132.
- McCulloh, T. H., J. R. Kandle, and J. E. Schoellhamer, 1968, Application of gravity measurements in Wells to problems of reservoir evaluation: 9th Annual Logging Symposium, Society of Professional well Log Analysts, Transactions, O1–O29.
- Meinesz, F. A. V., 1929, Theory and practice of pendulum observations at Sea: J. Waltman, Jr.
- Mendonça, C. A., and J. B. C. Silva, 1994, The equivalent data concept applied to the interpolation of potential field data: Geophysics, **59**, 722–732.
- , 1995, Interpolation of potential-field data by equivalent layer and minimum curvature: A comparative analysis: Geophysics, **60**, 399–407.
- Mesko, A., 1965, Some notes concerning the frequency analysis for gravity interpretation: Geophysical Prospecting, **13**, 475–488.
- Miller, H. G., and V. Singh, 1994, Potential field tilt: A new concept for location of potential field sources: Journal of Applied Geophysics, **32**, 213–217.
- Misener, D. J., F. S. Grant, and P. Walker, 1984, Variable depth, space-domain magnetic susceptibility mapping: 54th Annual International Meeting, SEG, Expanded Abstracts, 237.
- Moraes, R. A. V., and R. O. Hansen, 2001, Constrained inversion of gravity fields for complex 3D structures: Geophysics, **66**, 501–510.
- Moreau, F., D. Gibert, M. Holschneider, and G. Saracco, 1997, Wavelet analysis of potential fields: Inverse Problems, **13**, 165–178.
- Morelli, C., ed. 1974, The International Gravity Standardization Network 1971: International Association of Geodesy Special Publication 4.
- Moritz, H., 1980, Geodetic Reference System 1980: Journal of Geodesy, **54**, 395–405.
- Nabighian, M. N., 1972, The analytic signal of two-dimensional magnetic bodies with polygonal cross-section — Its properties and use for automated anomaly interpretation: Geophysics, **37**, 507–517.
- , 1974, Additional comments on the analytic signal of two-dimensional magnetic bodies with polygonal cross-section: Geophysics, **39**, 85–92.
- , 1984, Toward a three-dimensional automatic interpretation of potential field data via generalized Hilbert transforms — Fundamental relations: Geophysics, **49**, 780–786.
- Nagihara, S., and S. A. Hall, 2001, Three-dimensional gravity inversion using simulated annealing: Constraints on the diapiric roots of allochthonous salt structures: Geophysics, **66**, 1438–1449.
- Nagy, D., 1966, The gravitational attraction of a right rectangular prism: Geophysics, **31**, 362–371.
- Nettleton, L. L., 1939, Determination of density for reduction of gravimeter observations: Geophysics, **4**, 176–183.
- , 1942, Gravity and magnetic calculations: Geophysics, **7**, 293–310.
- Nettleton, L. L., L. J. B. LaCoste, and J. C. Harrison, 1960, Tests of an airborne gravity meter: Geophysics, **25**, 181–202.
- O'Brien, J., A. Rodriguez, and D. Sixta, 2005, Resolving the K-2 salt structure in the Gulf of Mexico: An integrated approach using prestack depth imaging and full tensor gravity gradiometry: The Leading Edge, **24**, 404–409.
- O'Connell, M. D., R. S. Smith, and M. A. Vallee, 2005, Gridding aeromagnetic data using longitudinal and transverse gradients with the minimum curvature operator: The Leading Edge, **24**, 142–145.
- Okabe, M., 1979, Analytical expressions for gravity anomalies due to homogeneous polyhedral bodies and translations into magnetic anomalies: Geophysics, **44**, 730–741.
- Oldenburg, D. W., 1974, The inversion and interpretation of gravity anomalies: Geophysics, **39**, 526–536.
- Opfer, R. P., and J. A. Dark, 1989, Application of GravStat to seismic statics and structural correction in Nevada: 59th Annual International Meeting, SEG, Expanded Abstracts, 1302–1304.
- Parker, R. L., 1972, The rapid calculation of potential anomalies: Geophysical Journal of the Royal Astronomical Society, **31**, 447–455.
- Parker, R. L., and K. D. Klitgord, 1972, Magnetic upward continuation from an uneven track: Geophysics, **37**, 662–668.
- Paterson, N. R., and C. V. Reeves, 1985, Applications of gravity and magnetic surveys: The state of the art in 1985: Geophysics, **50**, 2558–2594.
- Pawłowski, R. S., and R. O. Hansen, 1990, Gravity anomaly separation by Wiener filtering: Geophysics, **55**, 539–548.
- Pearson, W. C., 2001, Aeromagnetic imaging of fractures in a basin centered gas play: AAPG Explorer, **22**, no. 5, 52–55.
- Pedersen, L. B., 1977, Interpretation of potential field data — A generalized inverse approach: Geophysical Prospecting, **25**, 199–230.
- , 1979, Constrained inversion of potential field data: Geophysical Prospecting, **27**, 726–748.
- Peirce, J. W., and L. Lipkov, 1988, Structural interpretation of the Rukwa rift, Tanzania: Geophysics, **53**, 824–836 (discussion in Geophysics, **56**, 1499–1500, with reply by authors).
- Peirce, J. W., S. Sander, R. A. Charters, and V. Lavoie, 2002, Turner Valley, Canada — A case history in contemporary airborne gravity: 72nd Annual International Meeting, SEG, Expanded Abstracts, 783–787.
- Pepper, T. B., 1941, The Gulf underwater gravimeter: Geophysics, **6**, 34–44.
- Peters, L. J., 1949, The direct approach to magnetic interpretation and its practical application: Geophysics, **14**, 290–320.
- Phillips, J. D., 1996, Potential-field continuation: Past practice vs. modern methods: 66th Annual International Meeting, SEG, Expanded Abstracts, 1411–1414.
- , 2001, Designing matched bandpass and azimuthal filters for the separation of potential-field anomalies by source region and source type: 15th Geophysical Conference and Exhibition, Geophysicists, Australian Society of Exploration Expanded Abstracts, CD-ROM.
- Plouff, D., 1975, Derivation of formulas and FORTRAN programs to compute gravity anomalies of prisms: U. S. Department of Commerce National Technical Information Service Publication PB-243-526.
- , 1976, Gravity and magnetic fields of polygonal prisms and application to magnetic terrain corrections: Geophysics, **41**, 727–741.
- , 1977, Preliminary documentation for a FORTRAN program to compute gravity terrain corrections based on topography digitized on a geographic grid: U. S. Geological Survey Open-File Report 77-535.
- Popta, J. Van, J. M. T. Heywood, S. J. Adams, and D. R. Bostock, 1990, Use of borehole gravimetry for reservoir characterization and fluid saturation monitoring: Society of Petroleum Engineers, SPE20896.
- Pratsch, J. C., 1998, Gravity data define basin structure and the location of major oil and gas reserves: Examples from Subandean basins, Tunisia, and the U. S. Rocky Mountain region in R. I. Gibson, and P. S. Milligan, eds., Geologic applications of gravity and magnetics: Case histories: SEG Geophysical Reference Series 8 and AAPG Studies in Geology, **43**, 28–31.

- Pratson, L. F., R. E. Bell, R. N. Anderson, D. Dosch, J. White, C. Affleck, A. Grierson, B. E. Korn, R. L. Phair, E. K. Biegert, et al. 1998, Results from a high-resolution, 3-D marine gravity gradiometry survey over a buried salt structure, Mississippi Canyon area, Gulf of Mexico, *in* R. I. Gibson, and P. S. Millegan, eds., *Geologic applications of gravity and magnetics: Case histories: SEG Geophysical Reference Series 8 and AAPG Studies in Geology 43*, 137–145.
- Ransone, K., and E. E. Rosaire, 1936, The growth of company owned operations in Gulf Coast geophysical prospecting since July 1930: *Geophysics*, **1**, 306–312.
- Rapp, R. H., and Y. Yi, 1997, Role of ocean variability and dynamic topography in the recovery of the mean sea surface and gravity anomalies from satellite altimeter data: *Journal of Geodesy*, **71**, 617–629.
- Rasmussen, R., and L. B. Pedersen, 1979, End corrections in potential field modeling: *Geophysical Prospecting*, **27**, 749–760.
- Reamer, S. K., and J. F. Ferguson, 1989, Regularized two-dimensional Fourier gravity inversion method with application to the Silent Canyon caldera, Nevada: *Geophysics*, **54**, 486–496.
- Reigber, C., Z. King, R. König, and P. Schwintzer, 1996, CHAMP, a minisatellite mission for geopotential and atmospheric research: Spring Meeting, American Geophysical Union, Abstracts, S40.
- Ridsdill-Smith, T. A., 1998a, Separating aeromagnetic anomalies using wavelet matched filters: 68th Annual International Meeting, SEG, Expanded Abstracts, 550–553.
- , 1998b, Separation filtering of aeromagnetic data using filterbanks: *Exploration Geophysics*, **29**, 577–583.
- Ridsdill-Smith, T. A., and M. C. Dentith, 1999, The wavelet transform in aeromagnetic processing: *Geophysics*, **64**, 1003–1013.
- Robbins, S. L., 1981, Short note — Reexamination of the values used as constants in calculating rock density from borehole gravity data: *Geophysics*, **46**, 208–210.
- Roest, W. R., J. Verhoef, and M. Pilkington, 1992, Magnetic interpretation using the 3-D analytic signal: *Geophysics*, **57**, 116–125.
- Roy, A., 1958, Letter on residual and second derivative of gravity and magnetic maps: *Geophysics*, **23**, 860–861.
- Rybar, S., 1957, Eötövs torsion balance model E-54: *Geofisica Pura e Applicata*, **37**, 79–89.
- , 1923, The Eötövs torsion balance and its application to finding of mineral deposits: *Economic Geology*, **18**, 639–662.
- Saltus, R. W., and R. J. Blakely, 1983, HYPERMAG, an interactive, two-dimensional gravity and magnetic modeling program: U. S. Geological Survey Open-File Report 83-241.
- , 1993, HYPERMAG, an interactive, 2- and 2-1/2-dimensional gravity and magnetic modeling program, version 3.5: U. S. Geological Survey Open-File Report 93-287.
- Sandwell, D. T., and W. H. F. Smith, 1997, Marine gravity anomaly from Geosat and ERS-1 satellite altimetry: *Journal of Geophysical Research*, **102**, 10039–10054.
- , 2001, Bathymetric estimation, *in* L. L. Fu, and A. Cazenave, eds., *Satellite altimetry and earth sciences: Academic Press*, 441–457.
- Sandwell, D., S. Gille, J. Orcutt, and W. Smith, 2003, Bathymetry from space is now possible: EOS, *Transactions of the American Geophysical Union*, **84**, 37–44.
- Schultz, A. K., 1989, Monitoring fluid movement with the borehole gravity meter: *Geophysics*, **54**, 1267–1273.
- Schweydar, W., 1918, Die Bedeutung der Drehwaage von Eötövs für die geologische Forschung nebst Mitteilung der Ergebnisse einiger Messungen (The importance of the Eötövs torsion balance for geologic research and a report on the results of some measurements): *Zeitschrift für Praktische Geologie*, **26**, 157–162.
- Sharpton, V. L., R. A. F. Grieve, M. D. Thomas, and J. F. Halpenny, 1987, Horizontal gravity gradient — An aid to the definition of crustal structure in North America: *Geophysical Research Letters*, **14**, 808–811.
- Silva, J. B. C., and G. W. Hohmann, 1984, Airborne magnetic susceptibility mapping: *Exploration Geophysics*, **15**, 1–13.
- Simpson, R. W., R. C. Jachens, and R. J. Blakely, 1983, AIRYROOT: A FORTRAN program for calculating the gravitational attraction of an Airy isostatic root out to 166.7 km: U. S. Geological Survey Open-File Report 83-883.
- Simpson, R. W., R. C. Jachens, R. J. Blakely, and R. W. Saltus, 1986, A new isostatic gravity map of the conterminous United States with a discussion on the significance of isostatic residual anomalies: *Journal of Geophysical Research*, **91**, 8348–8372.
- Skeels, D. C., 1947, Ambiguity in gravity interpretation: *Geophysics*, **12**, 43–56.
- , What is residual gravity?: *Geophysics*, **32**, 872–876.
- Smith, N. J., 1950, The case for gravity data from boreholes: *Geophysics*, **15**, 605–636.
- Spector, A., 1968, Spectral analysis of aeromagnetic data: Ph.D. dissertation, University of Toronto.
- Spector, A., and F. S. Grant, 1970, Statistical models for interpreting aeromagnetic data: *Geophysics*, **35**, 293–302 (discussion and reply — **36**, 617 and **39**, 112; errata — **36**, 448 and **42**, 1563).
- Spieß, F. N., and G. L. Brown, 1958, Tests of a new submarine gravity meter: EOS — *Transactions of the American Geophysical Union*, **39**, 391–396.
- Sprenke, K. F., and E. R. Kanasewich, 1982, Gravity modeling in western Canada: 52nd Annual International Meeting, SEG, Expanded Abstracts, 250–252.
- Stewart, R. H., 1985, *Methods of satellite oceanography: University of California Press*.
- Swick, C. H., 1931, Determination of “g” by means of the free swinging pendulum, *in* The figure of the earth: National Research Council Bulletin 78, 151–166.
- Syberg, F. J. R., 1972a, A Fourier method for the regional-residual problem of potential fields: *Geophysical Prospecting*, **20**, 47–75.
- , 1972b, Potential field continuation between general surfaces: *Geophysical Prospecting*, **20**, 267–282.
- Talwani, M., 1998, Errors in the total Bouguer reduction: *Geophysics*, **63**, 1125–1130.
- , 2003, The Apollo 17 gravity measurements on the moon: The Leading Edge, **22**, 786–789.
- Talwani, M., and M. Ewing, 1960, Rapid computation of gravitational attraction of three-dimensional bodies of arbitrary shape: *Geophysics*, **25**, 203–225.
- Talwani, M., J. L. Worzel, and M. Landisman, 1959, Rapid gravity computations for two-dimensional bodies with application to the Mendocino submarine fracture zone: *Journal of Geophysical Research*, **64**, 49–59.
- Tapley, B., and M.-C. Kim, 2001, Applications to geodesy, *in* L.-L. Fu and A. Cazenave, eds., *Satellite altimetry and earth sciences: Academic Press*, 371–403.
- Tapley, B., C. Reigber, and W. Melbourne, 1996, Gravity recover and climate experiment (GRACE): Spring meeting, American Geophysical Union.
- Thompson, L. G. D., and L. J. B. LaCoste, 1960, Aerial gravity measurements: *Journal of Geophysical Research*, **65**, 305–322.
- Thurston, J. B., and R. J. Brown, 1994, Automated source-edge location with a new variable-pass horizontal gradient operator: *Geophysics*, **59**, 546–554.
- Tomoda, Y., J. Segawa, and T. Takemura, 1972, Comparison measurements of gravity at sea using a TSSG and a Graf-Askania sea gravimeter: *Journal of Physics of the Earth*, **20**, 267–270.
- Torge, W., 1989, *Gravimetry: Walter de Gruyter*.
- Vajk, R., 1956, Bouguer corrections with varying surface density: *Geophysics*, **21**, 1004–1020.
- Valliant, H. D., 1991, Gravity meter calibration at LaCoste and Romberg: *Geophysics*, **56**, 705–711.
- von Frese, R. R. B., W. J. Hinze, and L. W. Braile, 1981, Spherical earth gravity and magnetic anomaly analysis by equivalent point source inversion: *Earth and Planetary Science Letters*, **53**, 69–83.
- Watts, A., and J. Fairhead, 1999, A process-oriented approach to modeling the gravity signature of continental margins: The Leading Edge, **18**, 258–263.
- Webring, M., 1985, SAKI: A Fortran program for generalized linear inversion of gravity and magnetic profiles: U. S. Geological Survey, Open-File Report 85-122.
- Wenzel, H.-G., 1985, Hochausflösende Kugelfunktionsmodelle für das Gravitationspotential der Erde (High-precision spherical harmonic model for the gravitational potential of the earth): *University of Hanover Scientific Works Series 137*.
- Wing, C. G., 1969, MIT vibrating string surface-ship gravimeter: *Journal of Geophysical Research*, **74**, 5882–5894.
- Wolf, H., 1972, Lokale gravimetrische Bestimmung von Schwere-Horizontalableitungen (Local gravity-field estimates from horizontal derivatives): *Deutsche Geodätische Kommission Report 194*.
- Won, I. J., V. Murphy, P. Hubbard, A. Oren, and K. Davis, 2004, Geophysics and weapons inspection: The Leading Edge, **23**, 658–662.
- Woollard, G. P., 1943, A transcontinental gravitational and magnetic profile of North America and its relation to geologic structure: *Geological Society of America Bulletin*, **54**, 747–790.
- , 1979, The new gravity system — Changes in international gravity base station values and anomaly values: *Geophysics*, **44**, 1352–1366.
- Woollard, G. P., and J. C. Rose, 1963, *International gravity measurements: SEG*.
- Worzel, J. L., 1965, *Pendulum gravity measurements at sea 1936–1959: John Wiley & Sons*.

- Wyckoff, R. D., 1941, The Gulf gravimeter: *Geophysics*, **6**, 13–33.
- Xia, J., D. R. Sprowl, and D. Adkins-Heljeson, 1993, Correction of topographic distortions in potential-field data: A fast and accurate approach: *Geophysics*, **58**, 515–523.
- Yale, M. M., D. T. Sandwell, and A. H. Herring, 1998, What are the limitations of satellite altimetry?: *The Leading Edge*, **17**, 73–76.
- Zhang, J., C. Y. Wang, Y. Shi, Y. Cai, W.-C. Chi, D. Dreger, W. B. Cheng, and Y. H. Yuan, 2004, Three-dimensional crustal structure of central Taiwan from gravity inversion with a parallel genetic algorithm: *Geophysics*, **69**, 917–924.
- Zhdanov, M. S., R. Ellis, and S. Mukherjee, 2004, Three-dimensional regularized focusing inversion of gravity gradient tensor component data: *Geophysics*, **69**, 925–937.
- Zorin, Y. A., B. M. Pismenny, M. R. Novoselova, and E. K. Turutanov, 1985, Decompensative gravity anomaly (in Russian): *Geologia i Geofizika*, **8**, 104–105.
- Zumberge, M. A., J. A. Hildebrand, J. M. Stevenson, R. L. Parker, A. D. Chave, M. E. Ander, and F. N. Spiess, 1991, A submarine measurement of the Newtonian gravitational constant: *Physical Review Letters*, **67**, 3051–3054.
- Zurflueh, E. G., 1967, Applications of two-dimensional linear wavelength filtering: *Geophysics*, **32**, 1015–1035.